

**NANOFLUID FLOW HEAT AND MASS TRANSFER
OVER A POROUS STRETCHING SHEET**

By

Khadeeja Afzal



A Dissertation submitted in partial fulfillment of the requirements
for the degree of Master of Philosophy in Mathematics

Supervised by

Dr. Asim Aziz

Department of Mathematics

School of Natural Sciences (SNS)

National University of Sciences and Technology (NUST)


Islamabad, Pakistan

© Khadeeja Afzal, 2016s

National University of Sciences & Technology**MASTER'S THESIS WORK**

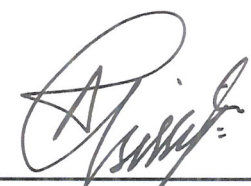
We hereby recommend that the dissertation prepared under our supervision by: Khadeeja Afzal, Regn No. NUST201463616MSNS78014F Titled: Nanofluid flow with heat and mass transfer over porous stretching sheet be accepted in partial fulfillment of the requirements for the award of **MS** degree.

Examination Committee Members1. Name: Dr. Moniba ShamsSignature: 2. Name: Dr. Muhammad Asif FarooqSignature: 3. Name: Dr. Noreen Sher AkbarSignature: 4. Name: Prof. Sohail NadeemSignature: Supervisor's Name: Dr. Asim AzizSignature: 


Head of Department

22-08-2016
Date

COUNTERSIGNEDDate: 22/8/16


Dean/Principal

Acknowledgement

In the name of Almighty Allah, the creator of everything, I am thankful to Him for blessing me and inspiring me with courage to do this work.

Firstly, I would like to express my sincerest gratitude and deepest regards to my supervisor *Dr. Asim Aziz*, Assistant Professor (EME) NUST, for providing precious time, encouragement, valuable guidance and continuous support during the entire period of thesis. I am extremely grateful to him for his constant support throughout my research phase with his knowledge which enabled me to complete my thesis work. His pleasant and committed nature along with energetic endorsement was a source of inspiration for me to complete this thesis.

My sincere gratitude is to my GEC members, Dr. Muhammad Asif Farooq (SNS) NUST, Dr. Noreen Sher Akbar (EME) NUST and Dr. Moniba Shams (SNS) NUST, for their guidance and support that helped me in completing this thesis in time.

My heartiest and sincere salutations to my parents Mr. Muhammad Afzal and Mrs. Nighat Yasmeen for the endless love, prayers and encouragement. I also feel grateful to my dearest siblings Ibrahim, Hajra and Nayab, for their endless moral support and continuous encouragement throughout the research work. I also acknowledge my dear friends Rida Ahmad, Hira Siddique, Ghulam Kubra and Laraib Hanif from the core of my heart for their help, sustenance and effort at lifting me up whenever, I was doleful. May Almighty Allah shower His choicest blessings and prosperity on all those who assisted me in any way during completion of my thesis.

Abstract

In this dissertation, the problem of an unsteady magnetohydrodynamics boundary layer slip flow with heat and mass transfer of nanofluids is investigated numerically. The analysis is carried on Cu-water and Al_2O_3 -water based nanofluids. The thermal conductivity of the nanofluid is assumed to be a function of temperature and slip conditions are employed in terms of the shear stress. The similarity transformations are used to transform the governing system of partial differential equations (PDEs) into a system of ordinary differential equations (ODEs) and then solved numerically. The numerical values obtained for the velocity, temperature and concentration depend on nanofluid's volume concentration parameter, unsteadiness parameter, thermal conductivity parameter, slip parameters, magnetic parameter and thermal radiation parameter. The effects of various parameters on the flow, heat and mass transfer characteristics as well as on skin friction coefficient, Nusselt number and Sherwood number are presented and discussed through graphs and tables.

Table of Contents

1	Introduction	1
1.1	Literature Review	1
2	Preliminaries	5
2.1	Fluid and Fluid Flow	5
2.2	Laminar and Turbulent Flow	5
2.3	Steady and Unsteady Flow	6
2.4	Incompressible and Compressible Flow	6
2.5	Viscosity	7
2.6	Viscous and Non-Viscous Flow	7
2.7	Newtonian and Non-Newtonian Fluid	7
2.8	Continuity Equation	8
2.9	Momentum Equation	8
2.10	Magnetohydrodynamics	9
2.11	Heat Transfer	10
2.11.1	Conduction	10
2.11.2	Convection	10
2.11.3	Radiation	11
2.12	Thermal Conductivity	11
2.13	Electrical Conductivity	11
2.14	Energy Equation	11
2.15	Mass Transfer	12
2.16	Concentration Equation	12

2.17	Reynolds Number (Re)	13
2.18	Prandtl Number (Pr)	13
2.18.1	Skin Friction Coefficient	13
2.19	Nusselt Number	13
2.19.1	Sherwood Number	14
2.19.2	Lewis Number	14
2.20	Slip Conditions	14
2.21	Nanofluid	14
2.21.1	Types of Nanofluid	15
2.21.2	Nanofluid's Physical Parameters	15
2.22	Similarity Transformation	15
3	Unsteady MHD Slip Flow and Heat Transfer of Nanofluids over a Porous Stretching Sheet	17
3.1	Problem Formulation	18
3.2	Method of Solution	20
3.3	Numerical Scheme of Solution	22
3.3.1	Verification of Numerical Results	22
3.4	Results and Discussion	23
3.4.1	Effect of Unsteadiness Parameter A	24
3.4.2	Effect of Volume Fraction Parameter ϕ	25
3.4.3	Effect of Velocity Slip parameter Λ	26
3.4.4	Effect of Thermal Slip parameter Ω	26
3.4.5	Effect of Magnetic Parameter M	27
3.4.6	Effect of Variable Thermal Conductivity Parameter ϵ	27
3.4.7	Effect of Radiation Parameter N_r	29
3.4.8	Effect of Suction Parameter $S > 0$ /Injection Parameter $S < 0$	29
4	Unsteady MHD Boundary Layer Slip Flow, Heat and Mass Transfer of Nanofluids over Porous Stretching Sheet	33
4.1	Problem Formulation	33

4.2	Method of Solution	34
4.3	Numerical Scheme of Solution	35
4.4	Results and Discussion	36
4.4.1	Effect of Unsteadiness Parameter A	37
4.4.2	Effect of Volume Fraction Parameter ϕ	37
4.4.3	Effect of Velocity Slip Parameter Λ	38
4.4.4	Effect of Concentration Slip Parameter δ	38
4.4.5	Effect of Lewis Number Le	39
4.4.6	Effect of Magnetic Parameter M	39
4.4.7	Effect of Suction Parameter $S > 0$ /Injection Parameter $S < 0$	40
5	Conclusions and Future Recommendations	44
	References	46

Chapter 1

Introduction

This chapter includes the basic introduction and brief literature review on boundary layer flow with heat and mass transfer of nanofluids over a stretching surface.

The boundary layer flow with the interaction of heat and mass transfer over a stretching surface has diverse applications in industry and technology. The applications of boundary layer theory include, but not limited to, the calculation of friction drag of a flat plate, a ship, an airfoil, the body of an airplane or a turbine blade, cooling devices, industrial flows such as conveyors etc.

1.1 Literature Review

Sakiadis [1] first solved the famous boundary layer equation for a continuously moving flat plate. Crane [2] extended the idea and studied the flow due to linearly stretching sheet. Thereafter, authors extensively studied the boundary layer flow including heat and mass transfer over a stretching sheet by considering parameters such as suction/injection, porosity, magnetic field, thermal radiation, viscous dissipation, joule heating, convective and slip boundary conditions (see [3–11]). Andersson [12, 13] studied the flow of non-Newtonian fluids over a stretching sheet including the effects of applied magnetic field. Whereas, Pop [14] studied the MHD flow over a stretching permeable surface. This work is further extended by Ganji *et al.* [15] and presented the analytical solution of MHD flow over a nonlinear stretching sheet. Elbashbeshy and Bazid [16] discussed the flow and heat

transfer analysis over an unsteady stretching surface. Ishak [17] analysed the unsteady MHD flow and heat transfer over a stretching plate and gave the numerical solution using similarity transformation technique. Ibrahim *et al.* [18] examined the influence of viscous dissipation and radiation on unsteady MHD mixed convection flow of micropolar fluids. Mukhopadhyay [19] included the effects of thermal radiation and porous medium on flow and heat transfer of fluid over an unsteady stretching sheet. Fang *et al.* [20] presented the unsteady stagnation point flow with mass transfer. Recently, Bhattacharyya [21] presented the heat transfer analysis of an unsteady boundary layer flow with unsteady temperature profile towards a shrinking/stretching sheet. Slip flow past a stretching surface was studied by Andersson [22]. Pal and Talukdar [23] did the perturbation analysis of an unsteady MHD convective heat and mass transfer in a boundary layer slip flow. Slip effects on MHD boundary layer flow over a stretching sheet were analysed by Mukhopadhyay [24]. Recently, Asim Aziz *et al.* in their work [25] examined the slip effects on steady boundary layer flow along with heat and mass transfer over a flat porous plate. Hayat *et al.* [26] studied unsteady MHD flow over an exponentially stretching sheet with slip conditions.

In order to model the flow and heat transfer at high temperature appropriately, it becomes essential to consider the variation in viscosity and thermal conductivity. Lai and Kulacki [27] considered the effects of variable viscosity on convective heat transfer along with a vertical surface in a porous medium. Pop *et al.* [28] presented the influence of variable viscosity on boundary layer flow and heat transfer due to a continuously moving flat plate. Chiam [29,30] in his work examined the effects of variable thermal conductivity on the boundary layer flow over a stretching sheet. Mukhopadhyay *et al.* [31,32] presented some significant investigations on the flow and heat transfer over a stretching sheet including the variable viscosity effects under different physical conditions. Recently, Hayat *et al.* [33] analysed numerically the effects of variable thermal conductivity on the mixed convective flow over a porous stretching surface subjected to the convective boundary conditions in the presence of uniform applied magnetic field.

Nanofluid is a new class of heat transfer fluid with enhanced thermal conductivity. Choi [34] for the first time coined the term nanofluid by introducing the nanoparticles in

the base fluids and theoretically demonstrated the feasibility of the concept of nanofluids. A comprehensive survey of convective transport in nanofluids was done by Buongiorno [35], who considered seven slip mechanisms that can produce a relative velocity between the nanoparticles and the base fluid. Nanofluids got an eminent scientific and engineering applications after Eastman *et al.* [36] extended the idea and studied an unusual thermal conductivity enhancement in copper (Cu) nanofluids at small nanoparticle volume fraction. Khan and Pop [37] first studied the boundary layer flow of a nanofluid past a stretching sheet and gave numerical results of the problem. The boundary layer flow induced in a nanofluid due to linearly stretching sheet was reported by Makinde and Aziz [38]. The MHD boundary layer flow of a nanofluid past vertical stretching permeable surface with suction/injection was investigated by Kandasamy *et al.* [39]. This work is further extended by Bhattacharya and Layek [40] while studying MHD boundary layer flow of nanofluid over an exponentially stretching permeable sheet. An unsteady MHD flow, heat and mass transfer over stretching sheet with a non-uniform heat source/sink is studied by Shankar and Yirga [41]. Nanofluid flow over an unsteady stretching surface in the presence of thermal radiation was studied by Kalidas *et al.* [42]. Effects of thermal radiation on boundary layer flow of nanofluids over a permeable stretching flat plate were discussed by Motsumi [43]. An unsteady MHD boundary layer flow of nanofluids with thermal radiation and viscous dissipation was observed by Shakhaoath *et al.* [44]. Nogrehabadi *et al.* [45] observed the effects of partial slip boundary conditions on the flow and heat transfer of nanofluids. Syahira and Anuar [46] analysed unsteady boundary layer flow of a nanofluid over a stretching sheet with a convective boundary condition. Zheng *et al.* [47] extended the idea and analysed the effects of velocity slip with temperature jump on MHD flow and heat transfer of nanofluid over a porous shrinking sheet. A list of the key references on boundary layer flow with slip condition can be found in [48]– [51]. Reddy *et al.* [52] carried out an analysis to investigate the influence of variable thermal conductivity and partial velocity slip on hydromagnetic two-dimensional boundary layer flow of nanofluid over a stretching sheet with convective boundary condition. Nogrehabadi *et al.* [53] carried out a comprehensive study on the effects of variable thermal conductivity and viscosity on the natural convective heat transfer of nanofluid over a

vertical plate. Recently, Rashid [54] worked on heat and mass transfer of MHD flow of nanofluid over a stretching sheet using quasi-linearization technique. MHD boundary layer flow of a nanofluid over an exponentially permeable stretching sheet with radiation and heat source/sink was studied by N. Kishan *et al.* [55]. A comprehensive literature survey on variable thermophysical properties of nanofluids is presented in [56]– [58].

Thesis contribution

In this thesis we have extended the previous investigations to study the slip effects on unsteady MHD boundary layer flow of nanofluid over a nonuniform porous stretching sheet. The governing system of partial differential equations (PDEs) is converted into a system of ordinary differential equations (ODEs) using similarity transformation technique and solved numerically. The computational results are discussed for various physical parameters effecting the flow, heat and mass transfer of the nanofluid.

This dissertation is divided as follow:

Chapter 2 contains basic definitions regarding the nanofluid flow. The basic governing equations for the fluid flow, continuity, momentum, energy and concentration are also introduced. These preliminary concepts are then employed in the subsequent chapters. In **Chapter 3** the slip effects on magnetohydrodynamic flow and heat transfer of nanofluids over a porous unsteady stretching sheet with variable thermal conductivity and thermal radiation are being discussed. The analysis is carried for Cu-water and Al_2O_3 -water nanofluids. The associated governing system of partial differential equations (PDEs) is transformed into a non-linear system of ordinary differential equations (ODEs), which is then solved numerically. The behaviour of physical parameters which influence the model is presented in the graphs and tables. In **Chapter 4** the study presented in chapter 3 is extended by including the mass transfer analysis of MHD nanofluid flow under slip conditions. **Chapter 5** summarizes the dissertation, gives the major results concluded from the entire research and recommendations for the future work.

Chapter 2

Basic Definitions

In this chapter basic definitions regarding the fluid flow, types of flow, and basic governing equations for fluid flow are stated. Heat transfer, modes of heat and mass transfer are also introduced. In addition an introduction to nanofluid, types and nanofluid's physical parameters are also delineated.

2.1 Fluid and Fluid Flow

A fluid is a substance that deforms continuously under the action of shearing forces, however small they may be. Liquids, gases, plasmas and some plastic solids are categorized as fluids. Motion of the fluid under unbalanced stresses is called fluid flow.

2.2 Laminar and Turbulent Flow

The fluid flow in which the particles move in smooth layers, or laminas is called laminar flow. In such flow, the path lines of fluid particles do not intersect each other. Turbulent flow is the flow in which velocity of the fluid particles at a given point changes continuously and they mix rapidly with each other along the path line due to their three dimensional velocity fluctuations.

2.3 Steady and Unsteady Flow

A flow in which the fluid properties at every point in a flow field remain constant with time variation is called steady flow. Mathematically, it is stated as

$$\frac{\partial \gamma}{\partial t} = 0, \quad (2.1)$$

where γ represents any fluid property.

A flow in which fluid's properties in a flow field vary with time is called unsteady flow, i.e.,

$$\frac{\partial \gamma}{\partial t} \neq 0. \quad (2.2)$$

2.4 Incompressible and Compressible Flow

A fluid flow in which density of the fluid remains constant is called an incompressible flow, i.e.,

$$\frac{D\rho}{Dt} = \frac{\partial \rho}{\partial t} + \mathbf{V} \cdot \nabla \rho = 0, \quad (2.3)$$

where $\rho = \frac{\text{mass}}{\text{volume}}$ denotes the fluid density and $\frac{D}{Dt}$ is the material derivative given by

$$\frac{D}{Dt} = \frac{\partial}{\partial t} + \mathbf{V} \cdot \nabla, \quad (2.4)$$

where \mathbf{V} is the velocity of the fluid flow and ∇ is the differential operator which in cartesian coordinate system is given by

$$\nabla = \frac{\partial}{\partial x} \hat{i} + \frac{\partial}{\partial y} \hat{j} + \frac{\partial}{\partial z} \hat{k}. \quad (2.5)$$

In equation (2.5) \hat{i} , \hat{j} and \hat{k} represent unit vectors in x, y and z directions, respectively.

Compressible flow is that in which density of the fluid does not remain constant, i.e.,

$$\frac{D\rho}{Dt} \neq 0. \quad (2.6)$$

Liquids are almost incompressible and gases are compressible fluids.

2.5 Viscosity

Viscosity is a physical property of fluid associated with shearing deformation of fluid particles when subjected to the applied forces. It measures resistance to the moving fluid by the applied shearing forces. Mathematically, it is stated as

$$\mu = \frac{\text{shear stress}}{\text{deformation rate}} \quad (2.7)$$

where μ is called the dynamic viscosity or absolute viscosity. Unit of dynamic viscosity in SI system is kg/ms and dimension $[ML^{-1}T^{-1}]$.

Kinematic viscosity (ν) is the ratio of dynamic viscosity to density of the fluid. Mathematically,

$$\nu = \frac{\mu}{\rho}. \quad (2.8)$$

Its SI unit is m^2/s and dimension $[L^2T^{-1}]$.

2.6 Viscous and Non-Viscous Flow

The fluid flow in which the internal viscous forces do not allow fluid to flow readily is called viscous flow. In non-viscous or inviscid flow the fluid flows due to negligible internal frictional forces.

2.7 Newtonian and Non-Newtonian Fluid

Fluids can be characterized as Newtonian and non-Newtonian based on their rheological behavior.

Newtonian fluids are characterized by Newton's law of viscosity; which states that shear stress varies linearly with the deformation rate. Mathematically,

$$\tau_{yx} = \mu \frac{du}{dy}, \quad (2.9)$$

where μ is the dynamic viscosity, du/dy is the deformation rate and τ_{yx} denotes the shear stress. Most common Newtonian fluids are water, air, gasoline and organic solvents. In contrast to the Newtonian-fluids, these fluids have non-linear relationship between stress

and deformation rate. These fluids obeys power-law. Mathematically, for unidirectional flow the power-law model is given by

$$\tau_{yx} = K\left(\frac{du}{dy}\right)^n, \quad (2.10)$$

$$= \eta \frac{du}{dy}, \quad (2.11)$$

where $\eta = K(du/dy)^{n-1}$ is the apparent viscosity, n is the flow behavior index and K is the consistency index. Most common fluids under this category are pastes, ketchup, blood and polymer solutions.

2.8 Continuity Equation

According to the law of conservation of mass, mass can neither be created nor be demolished but, can be transformed from one form to another. It suggests that if we consider the differential control volume system enclosed by a surface fixed in a space, then the mass inside a fixed control system will remain constant. The equation of continuity is be expressed as [59]

$$\frac{\partial \rho}{\partial t} + \nabla \cdot (\rho \mathbf{V}) = 0, \quad (2.12)$$

where $V = [u(x, y, z), v(x, y, z), w(x, y, z)]$ is the velocity field.

For incompressible flow, equation (2.12) becomes

$$\nabla \cdot \mathbf{V} = 0. \quad (2.13)$$

2.9 Momentum Equation

According to the Newton's second law of motion the generalized linear momentum equation for fluid particle is given by net force \mathbf{F} acting on a fluid particle equal to the time rate of change of linear momentum. Consider the system of control surface having infinitesimally small dimensions dx , dy and dz and a constant mass enclosed within the surface. For this system Newton's second law is

$$m \frac{D\mathbf{V}}{Dt} = F. \quad (2.14)$$

The law of conservation of momentum for fluid flow is given in ([59]) as

$$\rho \frac{D\mathbf{V}}{Dt} = \nabla \cdot \boldsymbol{\tau} + \rho b, \quad (2.15)$$

where $\boldsymbol{\tau}$ is the Cauchy stress tensor, $\nabla \cdot \boldsymbol{\tau} (= -\nabla P + \mu \nabla^2 V)$ represents surface forces and ρb gives the net body force. Equation (2.15) for newtonian fluids takes the form

$$\rho \left(\frac{\partial V}{\partial t} + (\mathbf{V} \cdot \nabla) V \right) = -\nabla P + \mu \nabla^2 V + \rho b. \quad (2.16)$$

2.10 Magnetohydrodynamics

Magnetohydrodynamics (MHD) is the branch of engineering in which the behaviour of magnetic field in electrically conducting fields is studied. The word magnetohydrodynamics is derived from magneto meaning magnetic field, hydro meaning liquid and dynamics stands for movement.

The set of equations which represents MHD flow is a combination of equations of motion and the Maxwell's equation of electromagnetism. The momentum equation (2.16) for the MHD fluid flow becomes

$$\rho \left(\frac{\partial V}{\partial t} + (\mathbf{V} \cdot \nabla) V \right) = -\nabla P + \mu \nabla^2 V + (\mathbf{J} \times \mathbf{B}). \quad (2.17)$$

In the above equation, \mathbf{J} is the current density and $\mathbf{B} = \mathbf{B} + \mathbf{B}_i$ is the total magnetic field and \mathbf{B}_i is the induced magnetic field. Using small magnetic Reynold's number approximation for MHD flow, \mathbf{B}_i is considered to be negligible in comparison to external magnetic field.

By Ohm's law, current density \mathbf{J} is given as

$$\mathbf{J} = \sigma(\mathbf{E} + \mathbf{V} \times \mathbf{B}), \quad (2.18)$$

where σ is the electrical conductivity and \mathbf{E} is the electrical field which is assumed to be negligible. Equation (2.18) is simplified as

$$\mathbf{J} \times \mathbf{B} = -\sigma B^2 V, \quad (2.19)$$

Using equation (2.19) the momentum equation (2.17) becomes

$$\rho \frac{D\mathbf{V}}{Dt} = -\nabla P + \mu \nabla^2 V - \sigma B^2 V. \quad (2.20)$$

2.11 Heat Transfer

Heat transfer is the thermal exchange of energy between physical systems. Whenever there is a temperature difference between physical systems heat transfer must take place. Heat transfer between systems can take place through three different ways, Conduction, Convection, Radiation.

2.11.1 Conduction

Conduction is the process of heat transfer due to molecular collisions. The word "conduction" is repeatedly used for three different kinds of behaviour: Heat conduction, Electrical conduction and Sound conduction.

Fourier proposed that heat transfer rate per unit area varies directly with temperature gradient, i.e.,

$$\frac{Q}{A} = -\kappa \frac{dT}{dx}. \quad (2.21)$$

In the above equation, κ is the constant of proportionality known as thermal conductivity, Q is the heat transfer rate, A is the area and dT/dx is the temperature gradient. The equation (2.21) is known as Fourier's Law.

2.11.2 Convection

Convection refers to the movement of fluid particles from the region of high thermal energy to the region of low thermal energy. In fluid dynamics, convection is the energy transfer due to bulk fluid motion. Convective heat transfer arises between a fluid in a motion and a bounding surface. Convective heat transfer depends upon the nature of the flow. Therefore convection has three forms: Forced convection, Natural (free) convection, Mixed convection. Heat transfer mechanism given by Newton's law of cooling as

$$\frac{Q}{A} = h(T_s - T_f), \quad (2.22)$$

where, h is the heat transfer coefficient, T_s and T_f represent the temperature of the object's surface and that of the environment, respectively.

2.11.3 Radiation

Radiation is the transfer of heat energy when it is carried by photons of light in the infrared and visible portion of electromagnetic spectrum. All bodies constantly emit thermal energy by the process of radiation. It does not require any medium for its transmission.

2.12 Thermal Conductivity

The intrinsic property of a material that relates its ability to conduct heat is called thermal conductivity. Mathematically, it is stated as

$$\kappa = \frac{Q\nabla L}{A\nabla T}, \quad (2.23)$$

where Q measures the quantity of heat transmitted through the unit length ∇L per unit area A and ∇T is the unit temperature gradient.

2.13 Electrical Conductivity

Electrical conductivity is defined as the ability of a material to allow the flow of electric current. Mathematically, it is given as

$$\sigma = \frac{l}{RA}, \quad (2.24)$$

where l , R and A represent length, resistance and area of the material, respectively. The SI unit of electrical conductivity is siemens per meter (S/m).

2.14 Energy Equation

First law of thermodynamics suggests that the rate of change of energy of fluid inside a control volume is equal to the rate of heat addition plus the rate of work done. The energy equation is given by the total change in energy as a result of net heat conduction and the work done by the stresses. Thus the simplest form of heat equation is

$$\frac{De}{Dt} = -\nabla q + H, \quad (2.25)$$

where $e(= \rho C_p T)$ represents the amount of heat per unit volume and $q = -\kappa \nabla T$ is the heat flux. The governing equation for conservation of energy can then be written as

$$\rho C_p \left(\frac{\partial T}{\partial t} + (V \cdot \nabla) T \right) = \nabla \cdot (\kappa \nabla T) + H, \quad (2.26)$$

where T is temperature of the fluid, C_p is the specific heat (energy per unit mass per degree Kelvin) at constant temperature, κ is the thermal conductivity, and H is a source term for the heat that can be generated in a region by different ways, like radioactive decay, viscous dissipation and shear heating etc.

2.15 Mass Transfer

The relative motion of chemical species from one region to another due to the concentration gradient is called mass transfer. Mass transfer by diffusion is the same as heat transfer by conduction. Heat and mass transfer are kinetic processes that can be studied separately or jointly. In case of diffusion-convection phenomenon, it is efficient to couple heat and mass transfer equations.

2.16 Concentration Equation

The law of conservation of concentration is defined as ([59])

$$\frac{DC}{Dt} = -\nabla \cdot \vec{K} + G, \quad (2.27)$$

where $C(x,y,z)$ is a concentration field in moles (or grams) per unit volume, \vec{K} is diffusion flux in moles per unit area per unit time and G is a source term due to chemical, nuclear, or other factors.

The Fick's first law states that the diffusion flux is proportional to the negative concentration gradient, i.e.,

$$\vec{K} = -D \nabla C, \quad (2.28)$$

where D is a constant of proportionality known as diffusivity. Substituting equation (2.28) into equation (2.27) we get the following form of governing concentration equation

$$\frac{\partial C}{\partial t} + (V \cdot \nabla) C = D \nabla^2 C + G. \quad (2.29)$$

2.17 Reynolds Number (Re)

Reynolds number is a dimensionless number defined as the ratio of inertial forces to the viscous forces.

$$Re = \frac{\frac{\rho U^2}{L}}{\frac{\mu U}{L^2}} = \frac{LU}{\nu}, \quad (2.30)$$

where, U is the free stream velocity and L is the characteristic length.

It is used to identify the different flow behaviors like laminar or turbulent flow. At low Reynolds number laminar flow arises, where viscous forces are dominant. At high Reynolds number the flow is turbulent, where inertial forces are preeminent.

2.18 Prandtl Number (Pr)

Prandtl number is a dimensionless number which is defined as the ratio of momentum diffusivity (ν) to the thermal diffusivity (α). Mathematically, it is written

$$Pr = \frac{\nu}{\alpha} = \frac{\frac{\mu}{\rho}}{\frac{\kappa}{\rho C_p}} = \frac{\mu C_p}{\kappa}. \quad (2.31)$$

2.18.1 Skin Friction Coefficient

Skin friction coefficient C_f measures the resistance between the fluid and solid surface. It is defined as

$$C_f = \frac{\tau_w}{\rho U_w^2}, \quad (2.32)$$

where U_w is the surface velocity and τ_w is the wall shear stress.

2.19 Nusselt Number

Nusselt number defines the ratio of convective to the conductive heat transfer at the surface of plate. Mathematically it is given as

$$Nu = \frac{qL}{\kappa}, \quad (2.33)$$

where q is the convective heat transfer coefficient and L is the characteristic length.

2.19.1 Sherwood Number

The Sherwood number Sh which is also called mass transfer Nusselt number is a ratio between rate of total mass transfer and the rate of mass transfer due to diffusion. It is defined as

$$Sh = \frac{Z}{D/L}, \quad (2.34)$$

where Z is the mass transfer coefficient and D is the mass diffusivity.

2.19.2 Lewis Number

Lewis number is a dimensionless number which is a measure of heat diffusion relative to mass diffusion. It gives relative magnitudes of heat and mass diffusion in the thermal and concentration boundary layers. Mathematically, it is given as

$$Le = \frac{\nu}{D}. \quad (2.35)$$

2.20 Slip Conditions

When the velocity, temperature and concentration of the fluid is different from that of the wall of the bounding surface through which the fluid is passing, the condition is referred as velocity slip, temperature slip and concentration slip, respectively.

2.21 Nanofluid

Nanofluid is a new class of heat transfer fluid with enhanced thermal conductivity. Nanofluid contains a base fluid and nano-sized (diameter less than 100 nm) material particles or fibers suspended in the ordinary fluids. The nanoparticles are actually made up of metals (Cu, Al, Ag), oxides ceramics (Al_2O_3 , CuO), nitride ceramics (AlN, SiN), carbide ceramics (SiC, TiC) and common base fluids are water, oil and ethylene glycol.

2.21.1 Types of Nanofluid

Based on nature of the base fluid (organic or inorganic) and the nanoparticles nanofluids can be categorized into different types like, process extraction nanofluids, environmental (pollutant-controlling nanofluids), bio-, pharmaceutical, polymer and drag-reduction nanofluids.

2.21.2 Nanofluid's Physical Parameters

Following Reddy *et al.* [52], the viscosity, density and specific heat capacity of the nanofluid are given as

$$\mu_{nf} = \frac{\mu_f}{(1 - \phi)^{2.5}}, \quad \rho_{nf} = (1 - \phi)\rho_f + \phi\rho_s, \quad (\rho C_p)_{nf} = (1 - \phi)(\rho C_p)_f + \phi(\rho C_p)_s, \quad (2.36)$$

where, ϕ is nanoparticle volume fraction coefficient, μ_f , ρ_f and $(C_p)_f$ are the dynamic viscosity, density and specific heat capacity of the base fluid, ρ_s and $(C_p)_s$ are the density and specific heat of the nanoparticles, respectively.

Maxwell [60] suggested that the thermal conductivity of the nanofluid κ_{nf} is a function of thermal conductivity of nanoparticles κ_s , conductivity of the base fluid κ_f and the volume fraction of nanoparticles ϕ . Similarly, the electrical conductivity of the nanofluid σ_{nf} is a function of electrical conductivity of nanoparticles σ_s , conductivity of the base fluid σ_f and the volume fraction of nanoparticles ϕ , i.e.,

$$\kappa_{nf} = \left[\frac{(\kappa_s + 2\kappa_f) - 2\phi(\kappa_f - \kappa_s)}{(\kappa_s + 2\kappa_f) + \phi(\kappa_f - \kappa_s)} \right] \kappa_f, \quad \sigma_{nf} = \left[1 + \frac{3\left(\frac{\sigma_s}{\sigma_f} - 1\right)\phi}{\left(\frac{\sigma_s}{\sigma_f} + 2\right) - \left(\frac{\sigma_s}{\sigma_f} - 1\right)\phi} \right] \sigma_f. \quad (2.37)$$

2.22 Similarity Transformation

Similarity transformation is a mathematical technique which reduces the number of independent variables of system of partial differential equations and convert it into a system of ordinary differential equations. It can be viewed as a rule for grouping the independent variables into a new variable. The following three steps are involved in generalized similarity transformation.

- Any continuous one-to-one transformation can be resolved into one or more basic transformation of the form

$$\xi = \xi(x), \quad \eta = \eta(x, y), \quad (2.38)$$

- The transformed equation in terms of independent variables (ξ, η) is required to satisfy the state requirements.
- Using similarity transformation the associated boundary conditions are also transformed and expressed in terms of new similarity variables.

Chapter 3

Unsteady MHD Slip Flow and Heat Transfer of Nanofluids over a Porous Stretching Sheet

This chapter includes the study of boundary layer flow and heat transfer of electrically conducting nanofluids (Cu-water and Al_2O_3 -water) over an unsteady stretching sheet. The analysis is carried out by considering temperature dependent thermal conductivity, radiative heat flux and slip boundary conditions. The thermal conductivity is considered to vary linearly with the temperature and slip conditions are employed in terms of shear stress. The governing system of partial differential equation (PDEs) is transformed into a system of nonlinear ordinary differential equations (ODEs) using similarity transformation, which is then solved numerically using MATLAB bvp4c code. The obtained numerical values for skin friction coefficient and Nusselt number, velocity and temperature are presented through graphs and tables. In sections (3.4.1) -(3.4.8) the effects of various parameters on the flow and heat transfer characteristics are discussed through graphs and tables.

3.1 Problem Formulation

Consider the unsteady magnetohydrodynamic flow of two dimensional, laminar and incompressible nanofluid over a non-uniform porous stretching surface. The surface of a sheet is moving with non-uniform velocity

$$U(x, t) = \frac{cx}{1 - \alpha t}. \quad (3.1)$$

The c is an initial stretching rate and $\frac{1}{1-\alpha t}$ ($\alpha t < 1$) is the effective stretching rate. The surface of the plate is insulated and admits partial slip condition. The leading edge of the plate is at $x = 0$ and coincides with the plane $y = 0$. The temperature of the plate is T_w and the temperature far away from the plate is T_∞ . The geometry of the flow model is given in Figure (3.1). The magnetic field $B(t) = \frac{B_o}{\sqrt{1-\alpha t}}$ is applied in the transverse direction to the plate and induced magnetic field is ignored by taking low Reynolds number approximation. In view of the above assumptions, as well as of the usual boundary layer approximations equations (2.13), (2.20) and (2.26) take the following form

$$\frac{\partial u}{\partial x} + \frac{\partial v}{\partial y} = 0, \quad (3.2)$$

$$\frac{\partial u}{\partial t} + u \frac{\partial u}{\partial x} + v \frac{\partial u}{\partial y} = \frac{\mu_{nf}}{\rho_{nf}} \frac{\partial^2 u}{\partial y^2} - \frac{\sigma_{nf} B^2(t) u}{\rho_{nf}}, \quad (3.3)$$

$$(\rho C_p)_{nf} \left(\frac{\partial T}{\partial t} + u \frac{\partial T}{\partial x} + v \frac{\partial T}{\partial y} \right) = \frac{\partial}{\partial y} \left(\kappa_{nf}^*(T) \frac{\partial T}{\partial y} \right) - \frac{\partial q_r}{\partial y}. \quad (3.4)$$

In equations (3.2)-(3.4), u and v are the velocities in x and y directions, respectively, t is time of the flow, μ_{nf} is dynamic viscosity of the nanofluid, ρ_{nf} is nanofluid density, σ_{nf} is electrical conductivity and $(C_p)_{nf}$ is specific heat capacity of the nanofluid as introduced in Chapter 2 and equation (2.36). In above equation (3.4) T is temperature of the nanofluid, $T_w(x, t) = T_\infty + \frac{cx}{1-\alpha t}$ is the sheet surface (wall) temperature and q_r is the radiative heat flux.

The corresponding boundary conditions are

$$u(x, 0) = U_w + A_1 \mu_{nf} \frac{\partial u}{\partial y}, \quad v(x, 0) = V_w, \quad T(x, 0) = T_w + D_1 \left(\frac{\partial T}{\partial y} \right), \quad (3.5)$$

$$u \rightarrow 0, \quad \text{as} \quad y \rightarrow \infty, \quad \text{and} \quad T \rightarrow T_\infty, \quad \text{as} \quad y \rightarrow \infty. \quad (3.6)$$

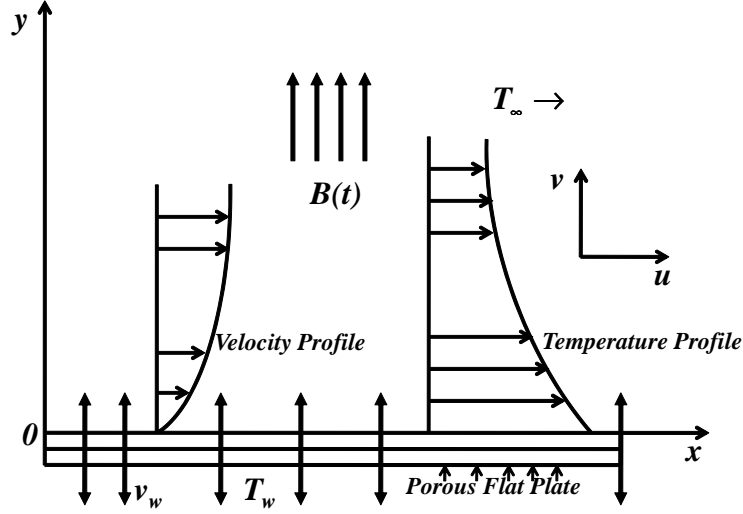


Figure 3.1: Geometry of the problem

Here V_w is constant suction/injection velocity with $V_w > 0$ for injection and $V_w < 0$ for suction, $A_1 = A_0\sqrt{1 - \alpha t}$ is the velocity slip factor and $D_1 = D_0\sqrt{1 - \alpha t}$ is the thermal slip factor with A_0 and D_0 be the initial values of velocity and thermal slip parameters, respectively. $\kappa_{nf}^*(T)$ is the temperature dependent thermal conductivity first introduced by Maxwell [60] as

$$\kappa_{nf}^*(T) = \kappa_{nf} \left(1 + \epsilon \frac{T - T_\infty}{T_w - T_\infty} \right), \quad (3.7)$$

where κ_{nf} is the thermal conductivity of the nanofluid and ϵ is the variable thermal conductivity parameter.

Using Rosseland approximation [61] for thermal radiation the radiative heat flux is simplified to

$$q_r = -\frac{4\sigma^*}{3k^*} \frac{\partial T^4}{\partial y}, \quad (3.8)$$

where k^* is the mean absorption coefficient and σ^* is the Stefan Boltzmann constant. It is assumed that the difference in temperature within the flow is such that T^4 can be represented as a linear combination of the temperature. Therefore, expanding T^4 in

Taylor's series about T_∞ and considering only the linear terms gives us

$$T^4 \cong 4T_\infty^3 T - 3T_\infty^4. \quad (3.9)$$

Equation (3.8) together with equation (3.9) becomes

$$\frac{\partial q_r}{\partial y} = -\frac{16T_\infty^3 \sigma^*}{3k^*} \frac{\partial^2 T}{\partial y^2}. \quad (3.10)$$

Substitution of equations (3.7) and (3.10) into equation (3.4) gives

$$(\rho C_p)_{nf} \left(\frac{\partial T}{\partial t} + u \frac{\partial T}{\partial x} + v \frac{\partial T}{\partial y} \right) = \frac{\partial}{\partial y} \left(\kappa_{nf} \left(1 + \epsilon \frac{T - T_\infty}{T_w - T_\infty} \right) \frac{\partial T}{\partial y} \right) + \frac{16T_\infty^3 \sigma^*}{3k^*} \frac{\partial^2 T}{\partial y^2}. \quad (3.11)$$

3.2 Method of Solution

In this section we transform the system of equations (3.2), (3.3) and (3.11) along with the boundary conditions (3.5) and (3.6) into a dimensionless form. For this purpose, the stream function $\psi(x, y)$ of the form

$$u = \frac{\partial \psi}{\partial y}, \quad v = -\frac{\partial \psi}{\partial x}, \quad (3.12)$$

identically satisfies the continuity equation (3.2). Using equation (3.12) equations (3.3) and (3.11) become

$$\begin{aligned} \frac{\partial^2 \psi}{\partial t \partial y} + \frac{\partial \psi}{\partial y} \frac{\partial^2 \psi}{\partial x \partial y} - \frac{\partial \psi}{\partial x} \frac{\partial^2 \psi}{\partial y^2} &= \frac{\mu_{nf}}{\rho_{nf}} \frac{\partial^3 \psi}{\partial y^3} - \frac{\sigma_{nf} B^2(t)}{\rho_{nf}} \frac{\partial \psi}{\partial y}, \quad (3.13) \\ (\rho C_p)_{nf} \left(\frac{\partial T}{\partial t} + \frac{\partial \psi}{\partial y} \frac{\partial T}{\partial x} - \frac{\partial \psi}{\partial x} \frac{\partial T}{\partial y} \right) &= \frac{\partial}{\partial y} \left(\kappa_{nf} \left(1 + \epsilon \frac{T - T_\infty}{T_w - T_\infty} \right) \frac{\partial T}{\partial y} \right) + \frac{16T_\infty^3 \sigma^*}{3k^*} \frac{\partial^2 T}{\partial y^2}. \quad (3.14) \end{aligned}$$

The boundary conditions are likewise transformed into the following form

$$\frac{\partial \psi}{\partial y} = U_w + A_1 \mu_{nf} \frac{\partial^2 \psi}{\partial y^2}, \quad \frac{\partial \psi}{\partial x} = -V_w, \quad T = T_w + D_1 \left(\frac{\partial T}{\partial y} \right), \quad \text{at } y = 0, \quad (3.15)$$

$$\frac{\partial \psi}{\partial y} \rightarrow 0, \quad T \rightarrow T_\infty, \quad \text{as } y \rightarrow \infty. \quad (3.16)$$

The introduction of dimensionless similarity variable, dimensionless stream function $\psi(\eta)$ and temperature $\theta(\eta)$ of the form

$$\eta = \sqrt{\frac{c}{v_f(1 - \alpha t)}} y, \quad \psi(x, y) = \sqrt{\frac{v_f c}{1 - \alpha t}} x f(\eta), \quad \theta(\eta) = \frac{T - T_\infty}{T_w - T_\infty}, \quad (3.17)$$

transforms the differential equations (3.13) and (3.14) to the form

$$f''' + (1-\phi)^{2.5} \left[(1-\phi + \phi \frac{\rho_s}{\rho_f}) \{ f f'' - f'^2 - A(f' + \frac{1}{2} f'' \eta) \} - M \left(1 + \frac{3(\frac{\sigma_s}{\sigma_f} - 1)\phi}{(\frac{\sigma_s}{\sigma_f} + 2) - (\frac{\sigma_s}{\sigma_f} - 1)\phi} \right) f' \right] = 0, \quad (3.18)$$

$$\theta'' \left(1 + \epsilon \theta + \frac{\kappa_f}{\kappa_{nf}} Pr Nr \right) + \epsilon \theta'^2 + Pr \frac{\kappa_f}{\kappa_{nf}} \left(1 - \phi + \phi \frac{(\rho C_p)_s}{(\rho C_p)_f} \right) [f \theta' - f' \theta - A(\theta + \frac{\eta}{2} \theta')] = 0, \quad (3.19)$$

where, $A = \frac{\alpha}{c}$, $Pr = \frac{\nu_f}{\alpha_f}$ is Prandtl number, $\alpha_f = \frac{\kappa_f}{(\rho C_p)_f}$ is thermal diffusivity of fluid, $Nr = \frac{16}{3} \frac{\sigma^* T_\infty^3}{\kappa^* \nu_f (\rho C_p)_f}$ is thermal radiation parameter and $M = \frac{\sigma_f B_0^2}{c \rho_f}$ is magnetic parameter.

The transformed boundary conditions (3.15) and (3.16) are

$$f(0) = S, \quad f'(0) = 1 + \frac{\Lambda}{(1-\phi)^{2.5}} f''(0), \quad \theta(0) = 1 + \Omega \theta'(0), \quad (3.20)$$

$$f'(\eta) \rightarrow 0, \quad \text{as} \quad \eta \rightarrow \infty, \quad \theta(\eta) \rightarrow 0, \quad \text{as} \quad \eta \rightarrow \infty. \quad (3.21)$$

In equations (3.20) and (3.21) $S = -V_w \sqrt{\frac{1-\alpha t}{\nu_f c}}$ is suction/injection parameter (with $S < 0$ for injection and $S > 0$ for suction), $\Lambda = A_0 \sqrt{\frac{c}{\nu_f}} \mu_f$ is first order velocity slip parameter, and $\Omega = D_0 \sqrt{\frac{c}{\nu_f}}$ is thermal slip parameter.

The important physical quantities of interest are skin friction coefficient and Nusselt number. The skin friction coefficient defined in section (2.18.1) with wall shear stress

$$\tau_w = -\mu_{nf} \left(\frac{\partial u}{\partial y} \right)_{y=0}, \quad (3.22)$$

is transformed into

$$C_f Re_x^{1/2} = -\frac{f''(0)}{(1-\phi)^{2.5}}. \quad (3.23)$$

Local Nusselt number Nu_x

$$Nu_x = \frac{x q_w}{\kappa_f (T_w - T_\infty)}, \quad (3.24)$$

with q_w defined as

$$q_w = -\kappa_{nf} \left(\frac{\partial T}{\partial y} \right)_{y=0}. \quad (3.25)$$

Equation (3.24) is transformed into

$$Nu_x Re_x^{-1/2} = -\theta'(0) \frac{\kappa_{nf}}{\kappa_f}. \quad (3.26)$$

3.3 Numerical Scheme of Solution

The transformed non dimensional governing equations (3.18) and (3.19) with conditions (3.20) and (3.21) are converted into simultaneous first order ordinary differential equations and then solved numerically by MATLAB built-in bvp4c solver. The resulting higher order ordinary differential equations are reduced to first order differential equations by taking

$$y_1 = f, \quad y_2 = f', \quad y_3 = f'', \quad y_4 = \theta, \quad y_5 = \theta'. \quad (3.27)$$

The non-linear differential equations (3.13) and (3.14) become

$$y_1' = y_2, \quad (3.28)$$

$$y_2' = y_3, \quad (3.29)$$

$$y_3' = -(1-\phi)^{2.5} \left[\left(1-\phi + \phi \frac{\rho_s}{\rho_f}\right) \{y_1 y_3 - y_2^2 - A(y_2 + \frac{\eta}{2} y_3)\} - M \left(1 + \frac{3(\frac{\sigma_s}{\sigma_f} - 1)\phi}{(\frac{\sigma_s}{\sigma_f} + 2) - (\frac{\sigma_s}{\sigma_f} - 1)\phi}\right) y_2 \right] = 0, \quad (3.30)$$

$$y_4' = y_5, \quad (3.31)$$

$$y_5' = \frac{1}{\left(1 + \frac{\kappa_f}{\kappa_{nf}} Nr + \epsilon y_4\right)} \left[Pr \frac{\kappa_f}{\kappa_{nf}} \left(1 - \phi + \phi \frac{(\rho C_p)_s}{(\rho C_p)_f}\right) \{A(y_4 + \frac{\eta}{2} y_5) + y_2 y_4 - y_1 y_5\} - \epsilon (y_5)^2 \right]. \quad (3.32)$$

The boundary conditions (3.20) and (3.21) become

$$y_1(0) = S, \quad y_2(0) = 1 + \frac{\Lambda}{(1-\phi)^{2.5}} y_3(0), \quad y_3(0) = a, \quad y_4(0) = 1 + \Omega y_5(0), \quad y_5(0) = b. \quad (3.33)$$

where \mathbf{a} and \mathbf{b} are unknown which are to be determined such that the boundary conditions $y_2(\infty)$ and $y_4(\infty)$ are satisfied.

3.3.1 Verification of Numerical Results

We have compared our results with Hayat [62] for several values of skin friction coefficient and Nusselt number by assuming $Pr = 1.0$, $Nr = 0.2667$, $\epsilon = 0.0$, $\Omega = 0.5$, and $\phi = 0.0$. The comparison is shown in Table (3.1) and the results are found to be in an excellent agreement. Thus, we are very much confident that the present results are accurate.

M	S	Λ	A	$-f''(0)$ Hayat [62]	$-f''(0)$ Present	$-\theta'(0)$ Hayat [62]	$-\theta'(0)$ Present
0.0				0.580873	0.580873	0.724131	0.724148
0.25	1.0	1.0	0.2	0.601575	0.601571	0.715271	0.715316
1.0				0.645009	0.645009	0.697184	0.697207
2.25				0.689086	0.689084	0.679832	0.679856
	0.0			0.557754	0.557753	0.460126	0.460508
1.0	0.2	1.0	0.2	0.575633	0.575634	0.501501	0.501691
	0.7			0.619717	0.619717	0.621022	0.621115
	1.0			0.645009	0.645009	0.697176	0.697207
		0.0		1.733191	1.73317	0.695134	0.695153
1.0	0.5	1.0	0.2	0.602285	0.602285	0.571204	0.57133
		5.0		0.175027	0.175027	0.491062	0.491301
		10.0		0.093228	0.0932284	0.471421	0.47152

Table 3.1: Comparison of values of $-f''(0)$ and $-\theta'(0)$ with that obtained by Hayat [62].

3.4 Results and Discussion

In this section, we discuss the numerical results presented in the form of graphs and tables. The computations are performed to study the effects of variation of unsteady parameter A , magnetic parameter M , velocity slip parameter Λ , thermal slip parameter Ω , thermal radiation Nr , variable thermal conductivity ϵ , suction/injection parameter S and volume fraction parameter ϕ on velocity and temperature profiles of Cu-water and Al_2O_3 -water nanofluids and demonstrated graphically in sections (3.4.1) - (3.4.8). The behaviour of skin friction coefficient and Nusselt number with the variation in physical parameters is shown in Tables (3.3) and (3.4).

The thermophysical properties of the base fluid water and the two different nanoparticles copper (Cu), Alumina (Al_2O_3) are given in Table (3.2).

Physical properties	Base fluid	Nanoparticle	Nanoparticle
	Water	Cu	Al ₂ O ₃
$C_p(J/kgK)$	4179	385	765
$\rho(kg/m^3)$	997.1	8933	3970
$k(W/mK)$	0.613	400	40
$\sigma(\Omega.m)^{-1}$	0.05	5.96×10^7	10^{-12}

Table 3.2: Thermophysical properties of the base fluid and nanoparticles.

3.4.1 Effect of Unsteadiness Parameter A

Figures (3.2) and (3.3) illustrate the influence of unsteady parameter A on velocity and temperature profiles. It is observed that the velocity decreases with the increase in A . The momentum boundary layer thickness decreases in result. Moreover, the velocity attains its maximum value near the surface and gradually decreases to zero at the free stream far away from the plate satisfying the boundary conditions thus, supporting the validity of the obtained numerical results. It is important to note that temperature is dependent on velocity in situations where heat transfer is accomplished by convection, as this principle will also be important for the following discussions. In Figure (3.3) the temperature profiles $\theta(\eta)$ decrease with the increase in unsteadiness parameter A for a given distance from the plate. The comparison of curves in Figures (3.2) and (3.3) shows

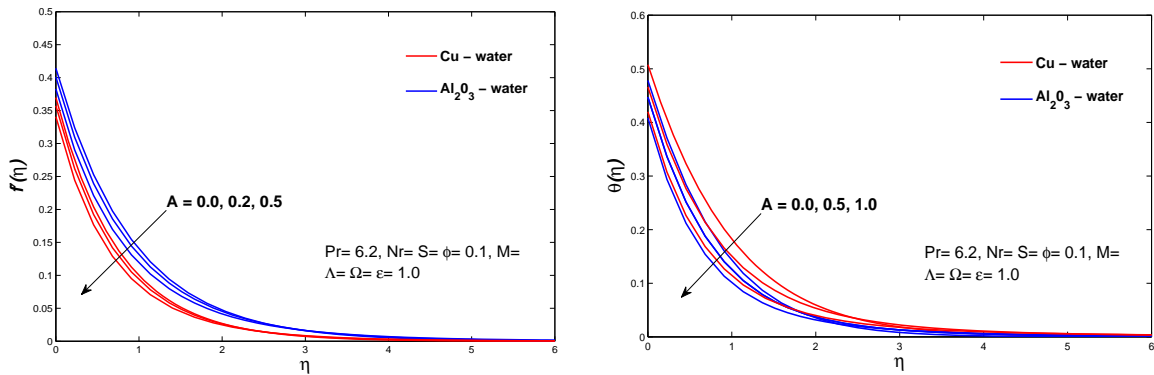


Figure 3.2: Velocity profiles for different values of unsteady parameter A .

Figure 3.3: Temperature profiles for different values of unsteady parameter A .

the impact of A on temperature profiles is more pronounced than that on the velocity profiles.

From Table (3.3), it is evident that values of skin friction coefficient increase with the increase in A , for both Cu-water and Al_2O_3 -water based nanofluids. Similarly, from Table (3.4) an increase in Nusselt number is observed with the increase in an unsteady parameter A .

3.4.2 Effect of Volume Fraction Parameter ϕ

The effect of variation of nanoparticle volume fraction ϕ on temperature and velocity profiles is illustrated in Figures (3.4) and (3.5), respectively. From Figure (3.4) it is observed that an increase in ϕ causes decrease in velocity profiles for Cu-water nanofluid. For Al_2O_3 -water nanofluid the behaviour is slight different i.e. near the surface (at about $\eta = 0.5$) the velocity profiles show the cross-over point. Before this point the velocity is decreasing and after this it starts increasing. Increase in ϕ causes an increase in temperature due to the fact that when the volume of nanoparticles increases, the thermal conductivity increases, which leads to the increase in thickness of thermal boundary layer. From Table (3.3), the increase in skin friction coefficient with the increase in volume

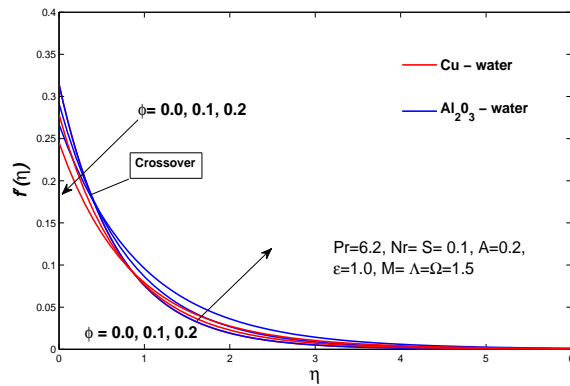


Figure 3.4: Velocity profiles for different values of volume fraction parameter ϕ .

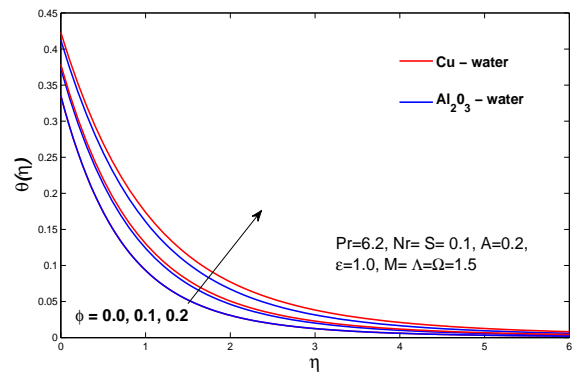


Figure 3.5: Temperature profiles for different values of volume fraction parameter ϕ .

friction parameter is observed for both the Cu-water and Al_2O_3 -water nanofluids. Table (3.4) shows the increase in Nusselt number with increase in volume fraction parameter.

3.4.3 Effect of Velocity Slip parameter Λ

The increase in first order velocity-slip parameter Λ causes decrease in velocity and increase in temperature as shown in Figures (3.6) and (3.7). The decrease in velocity is obvious from the increase in lubrication and slipperiness at the surface due to which the flow retards because the stretching pull can be only partly transmitted to the fluid. The increase in thermal boundary layer thickness is due to the fact that the fluid flow in the boundary layer due to stretching of the sheet.

It is observed from Table (3.3) that increase in Λ leads to decrease in skin friction coefficient both for Cu-water and Al_2O_3 -water nanofluids. As expected, the slip effects are to reduce the friction at the solid fluid interface and thus reduce skin friction coefficient. The reduction in Nusselt number is obvious from Table (3.4) by increasing Λ .

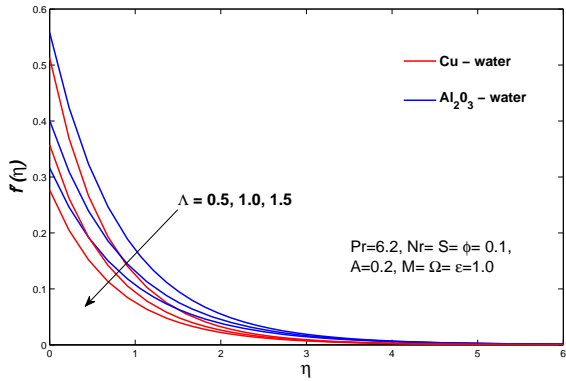


Figure 3.6: Velocity profiles for different values of velocity slip parameter Λ .

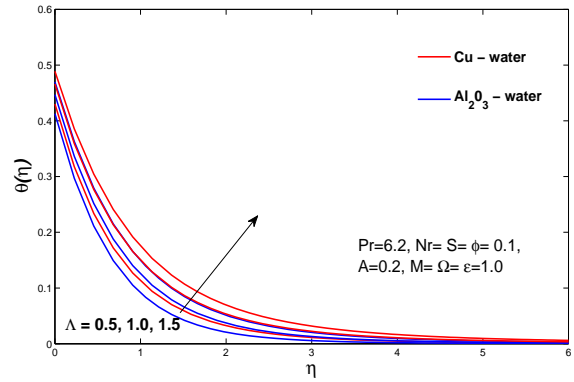


Figure 3.7: Temperature profiles for different values of velocity slip parameter Λ .

3.4.4 Effect of Thermal Slip parameter Ω

Figure (3.8) shows the reduction in the thickness of thermal boundary layer due to increase in thermal slip parameter. The increase in thermal slip parameter causes the less transfer of heat from sheet to the fluid which leads to the decrease in boundary layer temperature.

The temperature gradient at the surface decreases due to the thermal slip, and thus

decreases the Nusselt number as evident from Table (3.4), which represents the less heat transfer rate at the surface.

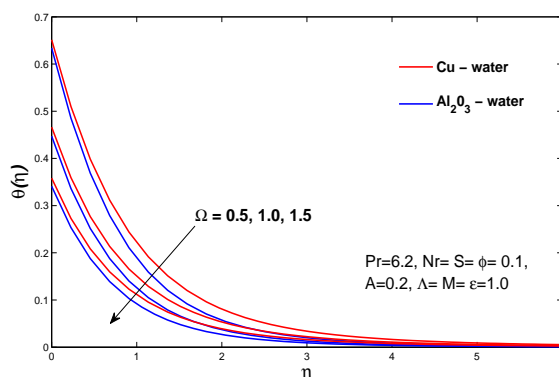


Figure 3.8: Temperature profiles for different values of thermal slip parameter Ω .

3.4.5 Effect of Magnetic Parameter M

The influence of magnetic parameter M on velocity and temperature profiles is shown in Figures (3.9) and (3.10), respectively. The increase in M causes decrease in velocity of the nanofluids. This is due to the fact that the applied transverse magnetic field produces a body force, called the Lorentz force, which resists the motion of the fluid. This causes decrease in thickness of the thermal boundary layer. Since magnetic parameter is inversely proportional to the density by $M = \frac{\sigma_f B_o^2}{c\rho_f}$, hence increase in M causes decrease in density and consequently, the temperature of the fluid rises.

From Table (3.3) we concluded that the skin friction coefficient increases with increase in M as expected due to the influence of the Lorentz force. The decrease in Nusselt number is observed with the increase in M from Table (3.4) due to the decrease in heat transfer rate.

3.4.6 Effect of Variable Thermal Conductivity Parameter ϵ

Thermal conduction is the spontaneous transfer of thermal energy from the region of high temperature to the region of low temperature. Figure (3.11) shows that increase in variable thermal conductivity parameter ϵ results in increase in thickness of thermal

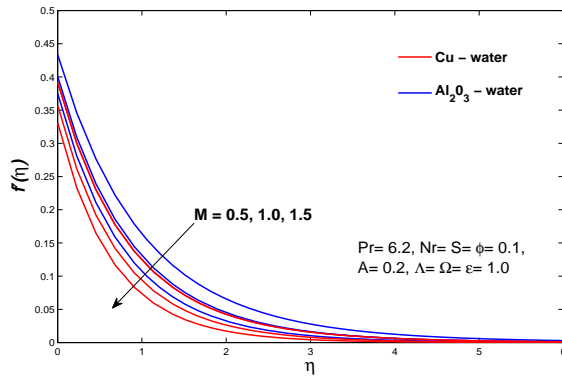


Figure 3.9: Velocity profiles for different values of magnetic parameter M .

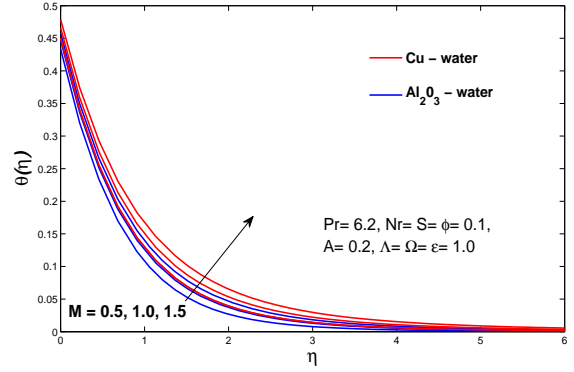


Figure 3.10: Temperature profiles for different values of Magnetic parameter M .

boundary layer. It is noticed that an increase in thermal conductivity parameter increases the fluid temperature across the boundary layer. This is because $\kappa_{nf}^* > \kappa_{nf}$ when $\epsilon > 0$ hence, an increasing ϵ results in increasing thermal conductivity, thereby raising the temperature. It would also increase the thermal boundary layer thickness. Furthermore,

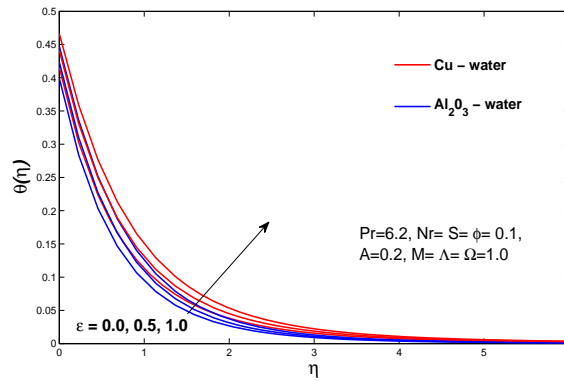


Figure 3.11: Temperature profiles for different values of variable thermal conductivity parameter ϵ .

it is observed from Table (3.4) that the Nusselt number decreases with the increase in ϵ because, large amount of heat transfer causes decrease in temperature gradient.

3.4.7 Effect of Radiation Parameter N_r

The effect of variation of thermal radiation parameter N_r is delineated in Figure (3.12). Thermal radiation parameter is the ratio of thermal radiation to the conductive radiation. Raising N_r depicts the dominance of thermal heat transfer over conductive heat transfer. Consequently, large amount of heat is transferred into the system, raising the temperature of the boundary layer. Increase in N_r leads to the decrease in the Nusselt number as observed from Table (3.3). This behaviour is true for both the Cu-water and Al_2O_3 water nanofluids.

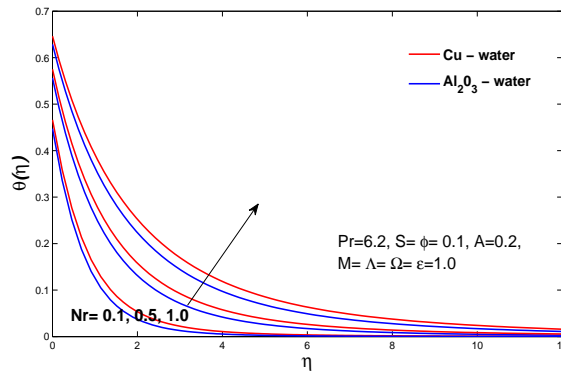


Figure 3.12: Temperature profiles for different values of thermal slip parameter N_r .

3.4.8 Effect of Suction Parameter $S > 0$ /Injection Parameter $S < 0$

Figures (3.13) - (3.16) demonstrate the effects of variation of suction/injection parameter on temperature and velocity profiles, respectively. Since applying suction leads to draw the amount of fluid particles into the wall hence, increase in S causes decrease in velocity of the nanofluid as shown in Figure (3.13). Opposite behavior is noted for injection ($S < 0$) in Figure (3.15). The physical explanation for such behavior is that as more fluid is injected, the heated fluid is pushed farther from the wall where due to less influence of the viscosity, the flow is accelerated.

It is observed from Figure (3.14) that increasing suction decreases temperature while increasing injection enhances it, as seen from Figure (3.16). Within the boundary layer

the momentum and thermal distributions are made uniform by applying the effects of suction and injection. Imposition of the suction on the surface causes reduction in the thermal boundary layer thickness whereas, the injection causes increase in it.

It can be seen from Tables (3.3) and (3.4) that the skin friction coefficient and the Nusselt number show the gradual reduction with the increase in injection parameter but, gradual rise with the increase in suction parameter.

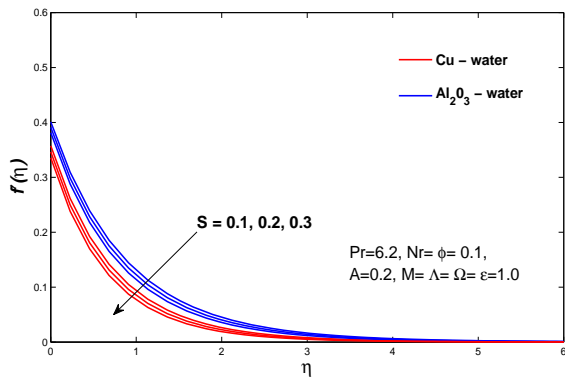


Figure 3.13: Velocity profiles for different values of suction parameter $S > 0$.

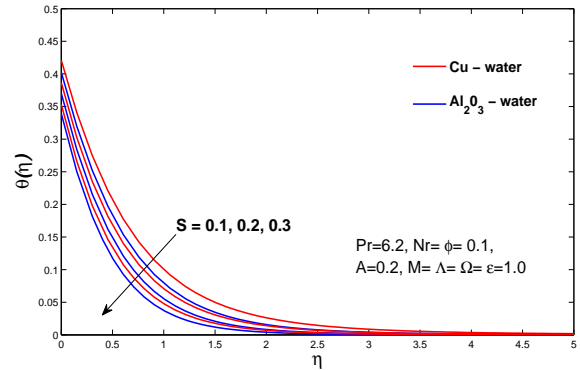


Figure 3.14: Temperature profiles for different values of suction parameter $S > 0$.

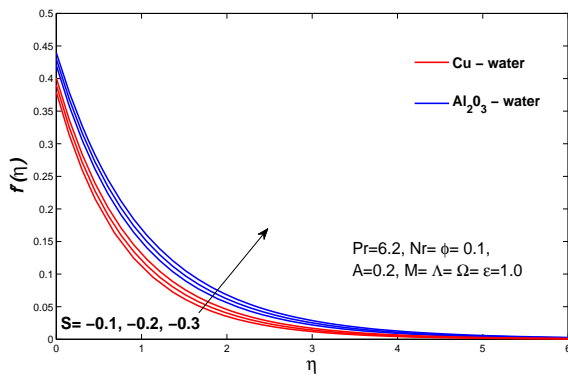


Figure 3.15: Velocity profiles for different values of injection parameter $S < 0$.

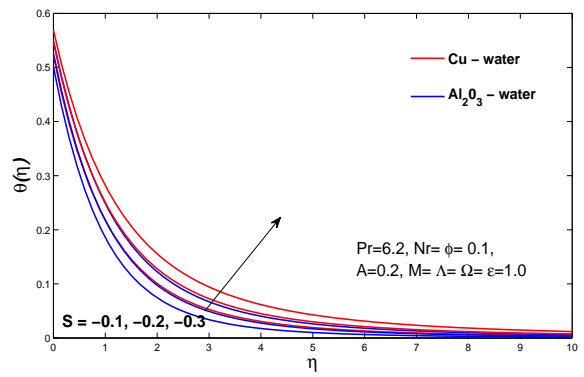


Figure 3.16: Temperature profiles for different values of injection parameter $S < 0$.

A	ϕ	Λ	Ω	M	ϵ	Nr	S	$-\frac{f''(0)}{(1-\phi)^{2.5}}$ <i>Cu - water</i>	$-\frac{f''(0)}{(1-\phi)^{2.5}}$ <i>Al₂O₃ - water</i>
0.0								0.630249	0.585716
0.2	0.1	1.0	1.0	1.0	1.0	0.1	0.1	0.642642	0.599083
0.5								0.659226	0.617033
	0.0							0.456858	0.456858
0.2	0.1	1.5	1.5	1.5	1.0	0.1	0.1	0.498264	0.472301
	0.2							0.531318	0.488702
		0.5						0.974604	0.88388
0.2	0.1	1.0	1.0	1.0	1.0	0.1	0.1	0.642642	0.599083
		1.5						0.482192	0.456043
				0.5				0.607699	0.566197
0.2	0.1	1.0	1.0	1.0	1.0	0.1	0.1	0.642642	0.599083
				1.5				0.668917	0.624708
							-0.1	0.759879	0.765432
0.2	0.1	1.0	1.0	1.0	1.0	0.1	-0.2	0.6099	0.569901
							-0.3	0.599049	0.560282
							0.1	0.642642	0.599083
0.2	0.1	1.0	1.0	1.0	1.0	0.1	0.2	0.653495	0.608837
							0.3	0.66425	0.618563

Table 3.3: Values of skin friction coefficient for the variation of parameters for fixed $Pr = 6.2$.

A	ϕ	Λ	Ω	M	ϵ	Nr	S	$-\theta'(0) \frac{\kappa_{nf}}{\kappa_f}$ <i>Cu - water</i>	$-\theta'(0) \frac{\kappa_{nf}}{\kappa_f}$ <i>Al₂O₃ - water</i>
0.0								0.655484	0.686876
0.2	0.1	1.0	1.0	1.0	1.0	0.1	0.1	0.710806	0.728076
0.5								0.772466	0.778936
	0.0							0.443119	0.443119
0.2	0.1	1.5	1.5	1.5	1.0	0.1	0.1	0.54032	0.550718
	0.2						0.2	0.644043	0.669053
		0.5						0.758684	0.773032
0.2	0.1	1.0	1.0	1.0	1.0	0.1	0.1	0.710806	0.728076
		1.5						0.68053	0.698121
			0.5					0.92843	0.964542
0.2	0.1	1.0	1.0	1.0	1.0	0.1	0.1	0.710806	0.728076
			1.5					0.569825	0.5787
				0.5				0.731951	0.745763
0.2	0.1	1.0	1.0	1.0	1.0	0.1	0.1	0.710806	0.728076
				1.5				0.693923	0.713231
					0.0			0.778698	0.791302
0.2	0.1	1.0	1.0	1.0	0.5	0.1	0.1	0.744205	0.759283
					1.0			0.710806	0.728076
						0.1		0.710806	0.728076
0.2	0.1	1.0	1.0	1.0	1.0	0.5	0.1	0.565924	0.584549
						1.0		0.4711	0.48884
							-0.1	0.637068	0.657116
0.2	0.1	1.0	1.0	1.0	1.0	0.1	-0.2	0.604018	0.624238
							-0.3	0.573973	0.593755
							0.1	0.710806	0.728076
0.2	0.1	1.0	1.0	1.0	1.0	0.1	0.2	0.749829	0.764538
							0.3	0.788742	0.800418

Table 3.4: Values of Nusselt number for the variation of parameters for fixed $Pr = 6.2$.

Chapter 4

Unsteady MHD Boundary Layer Slip Flow, Heat and Mass Transfer of Nanofluids over Porous Stretching Sheet

In this chapter we discuss the boundary layer flow with the interaction of heat and mass transfer of electrically conducting nanofluids (Cu-water and Al_2O_3 -water) over an unsteady stretching sheet. The focus of the present analysis is to study the effects of temperature dependent thermal conductivity, radiative heat flux and partial slip boundary conditions on velocity, temperature and concentration profiles of the nanofluids. The thermal conductivity is depending on the temperature and slip conditions are considered in terms of shear stress. The obtained numerical values for skin friction coefficient, Nusselt number, Sherwood's number, velocity, temperature and concentration are presented through graphs and tables.

4.1 Problem Formulation

In addition to equations (3.2) to (3.6) the present model includes the boundary layer concentration equation with slip condition. The concentration equation (2.29) under

boundary layer approximation becomes

$$\frac{\partial C}{\partial t} + u \frac{\partial C}{\partial x} + v \frac{\partial C}{\partial y} = D_B \frac{\partial^2 C}{\partial y^2}, \quad (4.1)$$

where C is the ambient concentration of the fluid and D_B is the Brownian diffusion coefficient.

The corresponding boundary conditions

$$C(x, 0) = C_w + K_1 \frac{\partial C}{\partial y}, \quad (4.2)$$

$$C \rightarrow C_\infty, \quad \text{as } y \rightarrow \infty. \quad (4.3)$$

In equations (4.2) and (4.3), $C_w(x, t) = C_\infty + \frac{cx}{1-\alpha t}$ is the nanoparticle volume fraction on the sheet surface, $K_1 = K\sqrt{1-\alpha t}$ is concentration slip parameter with K being initial value of concentration, and C_∞ is constant nanoparticle volume fraction at free stream.

4.2 Method of Solution

Introduction of stream function $\psi(x, y)$ given in the equation (3.12) will transform the equations (4.1) to (4.3) to

$$\frac{\partial C}{\partial t} + \frac{\partial \psi}{\partial y} \frac{\partial C}{\partial x} - \frac{\partial \psi}{\partial x} \frac{\partial C}{\partial y} = D_B \frac{\partial^2 C}{\partial y^2}, \quad (4.4)$$

$$C(x, 0) = C_w + K\sqrt{1-\alpha t} \frac{\partial C}{\partial y}, \quad (4.5)$$

$$C \rightarrow C_\infty, \quad \text{as } y \rightarrow \infty. \quad (4.6)$$

The dimensionless concentration variable $\beta(\eta)$ defined as,

$$\beta(\eta) = \frac{C - C_\infty}{C_w - C_\infty}, \quad (4.7)$$

transforms the differential equation (4.4) to the form

$$\beta'' + Le\{f\beta' - f'\beta - A(\beta + \frac{\eta}{2}\beta')\} = 0. \quad (4.8)$$

The transformed boundary conditions are

$$\beta(0) = 1 + \delta\beta'(0), \quad (4.9)$$

$$\beta(\eta) \rightarrow 0, \quad \text{as } \eta \rightarrow \infty. \quad (4.10)$$

In equation (4.9), $\delta = \sqrt{\frac{c}{\nu_f}} K$ is the concentration slip parameter.

Local Sherwood number Sh_x is defined as

$$Sh_x = \frac{xh_m}{D_B(C_w - C_\infty)}. \quad (4.11)$$

The mass flux h_m from the plate given as

$$h_m = -D_B \left(\frac{\partial C}{\partial y} \right)_{y=0}, \quad (4.12)$$

transforms equation (4.11) into

$$Sh_x Re_x^{-1/2} = -\beta'(0). \quad (4.13)$$

4.3 Numerical Scheme of Solution

The governing equations for the present model are (3.18), (3.19) and (4.8) along with the conditions (3.20), (3.21), (4.9) and (4.10). In order to solve the system numerically, we convert the higher order differential equations into a system of first order differential equations by taking

$$y_1 = f, \quad y_2 = f', \quad y_3 = f'', \quad y_4 = \theta, \quad y_5 = \theta', \quad y_6 = \beta, \quad y_7 = \beta'. \quad (4.14)$$

The corresponding higher order non-linear differential equations become

$$y_1' = y_2, \quad (4.15)$$

$$y_2' = y_3, \quad (4.16)$$

$$y_3' = -(1-\phi)^{2.5} \left[(1-\phi + \phi \frac{\rho_s}{\rho_f}) \{ y_1 y_3 - y_2^2 - A(y_2 + \frac{\eta}{2} y_3) \} - M \left(1 + \frac{3(\frac{\sigma_s}{\sigma_f} - 1)\phi}{(\frac{\sigma_s}{\sigma_f} + 2) - (\frac{\sigma_s}{\sigma_f} - 1)\phi} \right) y_2 \right] = 0, \quad (4.17)$$

$$y_4' = y_5, \quad (4.18)$$

$$y_5' = \frac{-1}{(1 + \epsilon y_4 + \frac{\kappa_f}{\kappa_{nf}} Nr)} \left[\epsilon (y_5)^2 + Pr \frac{\kappa_f}{\kappa_{nf}} \left\{ (1 - \phi + \phi \frac{(\rho C_p)_s}{(\rho C_p)_f}) \{ A(y_4 + \frac{\eta}{2} y_5) + y_2 y_4 - y_1 y_5 \} \right\} \right], \quad (4.19)$$

$$y'_6 = y_7, \quad (4.20)$$

$$y'_7 = Le\{y_2y_6 - y_1y_7 + A(y_6 + \frac{\eta}{2}y_7)\}, \quad (4.21)$$

with the initial conditions as :

$$y_1(0) = S, \quad (4.22)$$

$$y_2(0) = 1 + \frac{\Lambda}{(1 - \phi)^{2.5}}y_3(0), \quad (4.23)$$

$$y_3(0) = a_1, \quad (4.24)$$

$$y_4(0) = 1 + \Omega y_5(0), \quad (4.25)$$

$$y_5(0) = b_1, \quad (4.26)$$

$$y_6(0) = 1 + \delta y_7(0), \quad (4.27)$$

$$y_7(0) = c_1, \quad (4.28)$$

where, a_1 , b_1 , and c_1 being unknown are to be determined such that the boundary conditions $y_2(\infty)$, $y_4(\infty)$ and $y_6(\infty)$ are satisfied.

4.4 Results and Discussion

This section will discuss the numerical results of the analysis in the form of graphs and tables. The computations are performed to study the effects of variation of unsteady parameter, volume fraction parameter, slip parameters, magnetic parameter, thermal radiation, variable thermal conductivity, suction/injection parameter, and Lewis number Le on velocity, temperature and concentration profiles of Cu-water and Al_2O_3 -water nanofluids. It is observed that the velocity and temperature profiles for the present model are the same as discussed in the sections (3.4.1) - (3.4.8) so, here we will present only the concentration profiles to study the effects of various parameters. The behaviour of skin friction coefficient, Nusselt number and Sherwood number with the variation in physical parameters is shown in Tables (4.1)-(4.3).

4.4.1 Effect of Unsteadiness Parameter A

Figure (4.1) illustrates the influence of an unsteady parameter A on concentration profile. From Table(4.3) the increase in values of Sherwood number is observed with the increase in an unsteady parameter A , depicting the enhanced mass transfer rate.

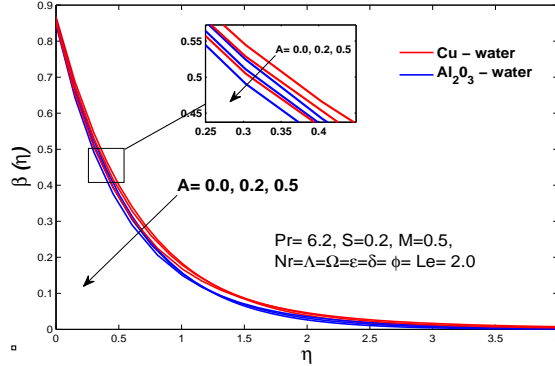


Figure 4.1: Concentration profiles for different values of unsteady parameter A .

4.4.2 Effect of Volume Fraction Parameter ϕ

Effect of variation of nanoparticle volume fraction ϕ on concentration profile is illustrated in Figure (4.2). Increase in ϕ causes increase in concentration as shown in Figure (4.2).

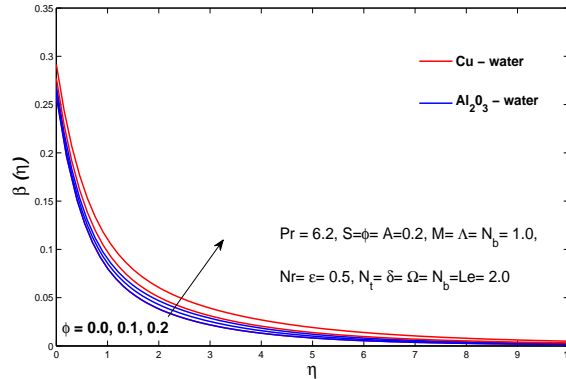


Figure 4.2: Concentration profiles for different values of volume fraction parameter ϕ .

Table(4.3) shows decrease in Sherwood number with increase in volume fraction parameter.

4.4.3 Effect of Velocity Slip Parameter Λ

The increase in first order velocity-slip parameter Λ causes increase in concentration profile as shown in Figure (4.3). Since the nanofluid slips over the bounding surface, it causes an increase in nanoparticle volume fraction within the boundary layer as observed from Figure (4.3).

It is observed from the Table (4.3) that increase in Λ leads to decrease in Sherwood number both for Cu-water and Al_2O_3 -water nanofluids showing the less mass transfer rate across the boundary.

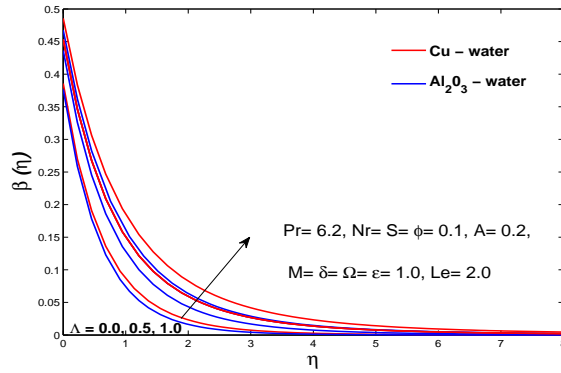


Figure 4.3: Concentration profiles for different values of velocity slip parameter Λ .

4.4.4 Effect of Concentration Slip Parameter δ

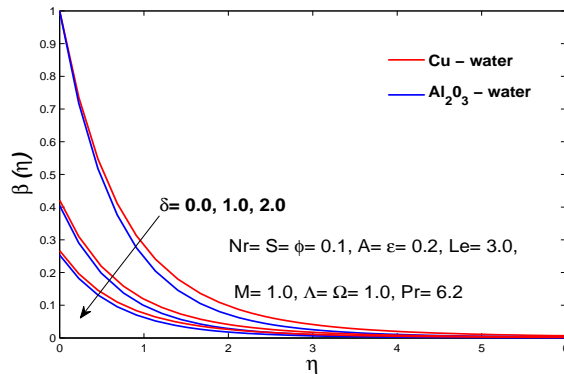


Figure 4.4: Concentration profiles for different values of concentration slip parameter δ .

Figure (4.4) depicts that the increasing δ has decreasing effect on concentration profiles. It can be seen from Table 4.3 that mass transfer rate shows gradual reduction by the variation of δ .

4.4.5 Effect of Lewis Number Le

Lewis number Le is defined as the ratio of thermal diffusivity to the mass diffusivity. As we increase the Lewis number the Brownian effect becomes prominent for which the concentration boundary layer thickness decreases as shown in Figure (4.5).

From Table (4.3) we concluded that increasing value of Le has increasing effect on Sherwood number.

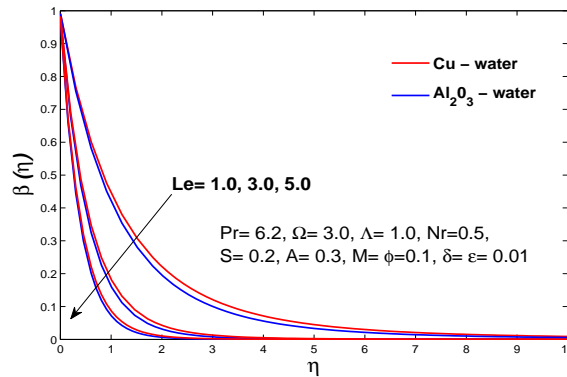


Figure 4.5: Concentration profiles for different values of Lewis number Le .

4.4.6 Effect of Magnetic Parameter M

Since the magnetic field produces a Lorentz force that opposes motion of the nanofluid due to which concentration across the boundary increases with the increase in M .

The decrease in Sherwood number is observed with the increase in M (4.3) due to influence of applied magnetic field.

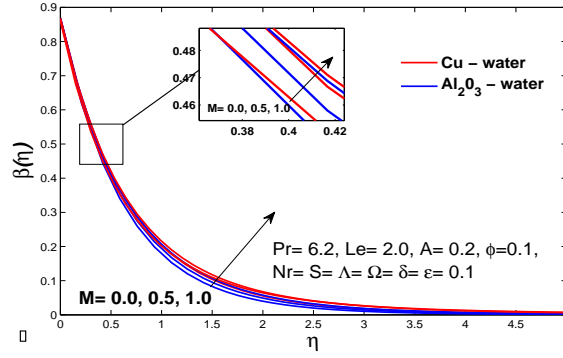


Figure 4.6: Concentration profiles for different values of magnetic parameter M .

4.4.7 Effect of Suction Parameter $S > 0$ /Injection Parameter $S < 0$

It is observed from Figure (4.7) that the concentration boundary layer thickness decreases with the increase in suction parameter since, we are drawing the nanofluid from the porous boundary which decreases the nanoparticle concentration within the boundary layer while it increases by increasing injection parameter as delineated in Figure (4.8). It can be seen from Table (4.3) that the Sherwood number shows gradual raise with the increase in suction parameter but gradual reduction with the increase in injection parameter

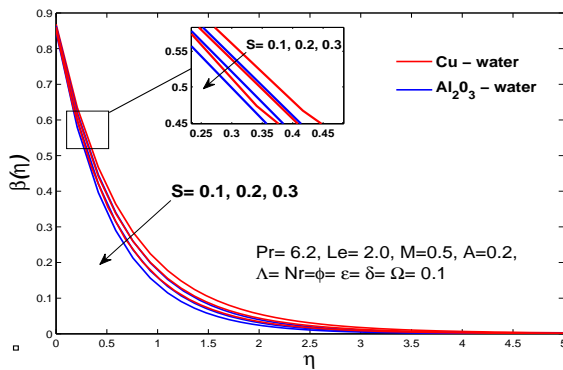


Figure 4.7: Concentration profiles for different values of suction parameter $S > 0$.

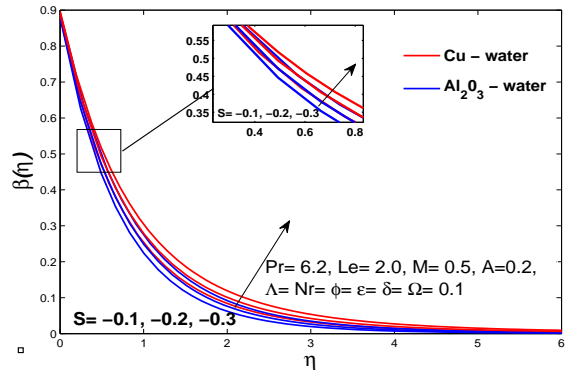


Figure 4.8: Concentration profiles for different values of injection parameter $S < 0$.

A	ϕ	Λ	Ω	δ	Le	M	ϵ	Nr	S	$-\frac{f''(0)}{(1-\phi)^{2.5}}$ <i>Cu - water</i>	$-\frac{f''(0)}{(1-\phi)^{2.5}}$ <i>Al₂O₃ - water</i>
0.0										1.57765	1.3471
0.2	0.1	0.1	0.1	0.1	2.0	0.5	0.1	0.1	0.2	1.64055	1.40449
0.5										1.73102	1.48711
	0.0									0.575634	0.575633
0.2	0.1	1.0	2.0	2.0	2.0	1.0	0.5	0.5	0.2	0.653494	0.608837
	0.2									0.715023	0.642842
		0.0								2.19094	1.81157
0.2	0.1	0.5	1.0	1.0	3.0	1.0	1.0	0.1	0.1	0.974604	0.88388
		1.0								0.642642	0.599083
						0.0				1.39419	1.21069
0.2	0.1	0.1	0.1	0.1	2.0	0.5	0.1	0.1	0.1	1.57672	1.35611
						1.0				1.73055	1.48114
									-0.1	1.4557	1.26395
0.2	0.1	0.1	0.1	0.1	2.0	0.5	0.1	0.1	-0.2	1.39866	1.22023
									-0.3	1.34398	1.17811
									0.1	1.57672	1.35611
0.2	0.1	0.1	0.1	0.1	2.0	0.5	0.1	0.1	0.2	1.64055	1.40449
									0.3	1.70647	1.45433

Table 4.1: Values of skin friction coefficient for the variation of parameters with fixed $Pr = 6.2$.

A	ϕ	Λ	Ω	δ	Le	M	ϵ	Nr	S	$-\theta'(0) \frac{\kappa_{nf}}{\kappa_f}$ <i>Cu - water</i>	$-\theta'(0) \frac{\kappa_{nf}}{\kappa_f}$ <i>Al₂O₃ - water</i>
0.0										2.21253	2.25919
0.2	0.1	0.1	0.1	0.1	2.0	0.5	0.1	0.1	0.2	2.30425	2.34323
0.5										2.43981	2.46751
	0.0									0.334251	0.334251
0.2	0.1	1.0	2.0	2.0	2.0	1.0	0.5	0.5	0.2	0.42167	0.427714
	0.2									0.523628	0.536738
		0.0								0.856228	0.856857
0.2	0.1	0.5	1.0	1.0	3.0	1.0	1.0	0.1	0.1	0.758684	0.773031
		1.0								0.710806	0.728075
			0.5							0.997271	1.03089
0.1	0.1	1.0	1.0	1.0	3.0	1.0	1.0	0.1	0.2	0.749828	0.764536
			1.5							0.594015	0.600904
						0.0				0.53502	0.531926
0.2	0.1	0.1	0.1	0.1	2.0	0.5	0.1	0.1	0.1	0.531729	0.529519
						1.0				0.528793	0.527345
							0.0			2.04913	2.09977
0.5	0.1	0.5	0.1	0.5	3.0	5.0	1.0	0.1	0.1	1.5309	1.57684
							2.0			1.25026	1.291060
								0.1		2.14664	2.18681
0.2	0.1	0.1	0.1	0.1	2.0	0.5	0.1	0.5	0.1	1.39018	1.43293
								1.0		1.01891	1.05915
									-0.1	1.85475	1.89433
0.2	0.1	0.1	0.1	0.1	2.0	0.5	0.1	0.1	-0.2	1.72269	1.76045
									-0.3	1.60089	1.63594
									0.1	2.14664	2.18681
0.2	0.1	0.1	0.1	0.1	2.0	0.5	0.1	0.1	0.2	2.30424	2.34322
									0.3	2.46785	2.50475

Table 4.2: Values of Nusselt number for the variation of parameters with fixed $Pr = 6.2$.

A	ϕ	Λ	Ω	δ	Le	M	ϵ	Nr	S	$-\beta'(0)$ <i>Cu - water</i>	$-\beta'(0)$ <i>Al₂O₃ - water</i>
0.0										1.32708	1.3856
0.2	0.1	0.1	0.1	0.1	2.0	0.5	0.1	0.1	0.2	1.39629	1.44783
0.5										1.49761	1.53974
	0.0									0.357859	0.357859
0.2	0.1	1.0	2.0	2.0	2.0	1.0	0.5	0.5	0.2	0.349817	0.356931
	0.2									0.343719	0.355841
		0.0								0.614282	0.623177
0.2	0.1	0.5	1.0	1.0	3.0	1.0	1.0	0.1	0.1	0.546627	0.563696
		1.0								0.514358	0.532563
				0.0						1.37299	1.47062
0.2	0.1	1.0	1.0	1.0	3.0	1.0	0.2	0.1	0.1	0.578591	0.595243
				2.0						0.366524	0.373136
					1.0					0.856688	0.902056
0.3	0.1	1.0	3.0	0.01	3.0	0.1	0.01	0.5	0.2	1.7259	1.80075
					5.0					2.40364	2.49471
						0.0				1.35751	1.39826
0.2	0.1	0.1	0.1	0.1	2.0	0.5	0.1	0.1	0.1	1.31448	1.36474
						1.0				1.27819	1.33558
									-0.1	1.16313	1.20926
0.2	0.1	0.1	0.1	0.1	2.0	0.5	0.1	0.1	-0.2	1.09423	1.1376
									-0.3	1.03009	1.1376
									0.1	1.31448	1.36474
0.2	0.1	0.1	0.1	0.1	2.0	0.5	0.1	0.1	0.2	1.39629	1.44783
									0.3	1.4816	1.53391

Table 4.3: Values of Sherwood's number number for the variation of parameters with fixed $Pr = 6.2$.

Chapter 5

Conclusions and Future Recommendations

In this thesis, we studied the MHD slip flow with heat and mass transfer of Cu-water and Al_2O_3 -water based nanofluids over a porous stretching sheet with variable thermal conductivity and thermal radiation. The significance of the current investigation is that the velocity, thermal and mass slip conditions are considered at the boundary and thermal conductivity is taken to vary linearly with the temperature.

We have drawn the following conclusions from our analysis:

1. Nanoparticles are known to enhance the thermal behaviour of the fluid. Increase in concentration of the nanoparticles enhances the temperature and concentration of the nanofluid. Nanoparticles volume fraction is found to increase the skin friction coefficient by decreasing the velocity of the nanofluid within the boundary layer.
2. In general, an increase in velocity slip parameter decreases the velocity and increases the temperature and mass transfer of nanofluids within the boundary layer. Thermal slip parameter reduces the thermal boundary layer thickness whereas, it has no effect on velocity and concentration of the nanofluids. Concentration slip has decreasing effect on mass transfer rate and renders the velocity and temperature profiles unchanged.
3. Unsteady parameter has same decreasing effect on velocity, temperature and con-

centration profiles of nanofluids. It increases the skin friction, heat and mass transfer rate across the boundary layer.

4. Magnetic field has pronounced effects on the nanofluid's physical profiles. Stronger magnetic field decreases the nanofluid's velocity and enhances the temperature and concentration at the boundary.
5. Temperature dependent thermal conductivity decreases the thermal boundary layer thickness hence, increases the heat transfer rate at the boundary. It's variation has no effect on velocity and concentration profiles.
6. Cu water nanofluids are better thermal conductors than Al_2O_3 water nanofluids under the considered assumptions.

The present model has revealed the significant results to focus on the slip effects, unsteadiness and temperature dependent thermal conductivity on the flow of nanofluids over a nonlinear porous stretching sheet. Future investigations may involve the study of the use of temperature dependent viscosity, variable porosity and multidimensional MHD slip flow and heat transfer of nanofluids. An interesting area to explore in future analysis would be the study of the above mentioned effects on the power-law and third grade fluid. Clearly, there is an opportunity for practical work on these systems.

References

- [1] B. Sakiadis, “Boundary layer equations for the two-dimensional and axi-symmetric flow,” *Journal of American Institute of Chemical Engineering*, vol. 7, pp. 26–28, 1961.
- [2] L. J. Crane, “Flow past a stretching plate,” *Zeitschrift fr angewandte Mathematik und Physik ZAMP*, vol. 21, pp. 645–647, 1970.
- [3] P. S. Gupta and A. S. Gupta, “Heat and mass transfer on a stretching sheet with suction or blowing,” *Canadian Journal of Chemical Engineering*, vol. 55, pp. 744–746, 1977.
- [4] C. Y. Wang, “The three dimensional flow due to a stretching flat surface,” *Physics of Fluids*, vol. 27, pp. 1915–1917, 1984.
- [5] C. Y. Wang, “Flow due to a stretching boundary with partial slip: an exact solution of the navier–stokes equations,” *Acta Mechanica*, vol. 57, pp. 3745–3747, 2002.
- [6] R. Nazar, N. Amin, D. Filip, and I. Pop, “Unsteady boundary layer flow in the region of the stagnation-point on a stretching sheet,” *International Journal of Engineering Science*, vol. 42, pp. 1241–1253, 2004.
- [7] M. J. Martin and I. D. Boyd, “Momentum and heat transfer in laminar boundary layer with slip flow,” *Journal of Thermophysics and Heat Transfer*, vol. 20, pp. 710–719, 2006.

- [8] K. V. Prasad, K. Vajravelu, and P. S. Datti, “The effects of variable fluid properties on the hydro-magnetic flow and heat transfer over a non-linearly stretching sheet,” *International Journal of Thermal Science*, vol. 49, pp. 603–610, 2010.
- [9] T. Hayat, M. Awais, M. Qasim, and A. Awatif, “Effects of mass transfer on the stagnation point flow of an upperconvected maxwell (ucm) fluid,” *International Journal of Heat and Mass Transfer*, vol. 54, pp. 3777–3782, 2011.
- [10] S. Nadeem, R. U. Haq, N. S. Akbar, C. Lee, and Z. H. Khan, “Numerical study of boundary layer flow and heat transfer of Oldroyd-B nanofluid towards a stretching sheet,” *PLOS ONE*, vol. 8, 2013.
- [11] M. Qasim, I. Khan, and S. Shafie, “Heat transfer in a micropolar fluid over a stretching sheet with newtonian heating,” *PLOS ONE*, vol. 8, 2013.
- [12] H. I. Andersson, “MHD flow of a visco-elastic fluid past a stretching surface,” *Acta Mechanica*, vol. 95, pp. 227–230, 1992.
- [13] H. I. Andersson, K. H. Bech, and B. S. Dandapat, “Magnetohydrodynamic flow of a power-law fluid over a stretching sheet,” *International Journal of Non-Linear Mechanics*, vol. 27, pp. 929–936, 1992.
- [14] I. Pop and T. N. Yen, “A note on mhd flow over a stretching permeable surface,” *Mechanics Research Communications*, vol. 25, pp. 263–269, 1998.
- [15] D. D. Ganji, H. Bararnia, S. Soleimani, and E. Ghasemi, “Analytical solution of the magneto-hydrodynamic flow over a nonlinear stretching sheet,” *Modern Physics Letters B*, vol. 23, no. 20-21, pp. 2541–2556, 2009.
- [16] E. M. A. Elbashbeshy and M. A. A. Bazid, “Heat transfer over an unsteady stretching surface,” *Heat and Mass Transfer*, vol. 41, pp. 1–4, 2004.
- [17] A. Ishak, “Unsteady mhd flow and heat transfer over a stretching plate,” *Journal of Applied Sciences*, vol. 10, no. 18, pp. 2127–2131, 2010.

- [18] F. S. Ibrahim, A. M. Elaiw, and A. A. Bakr, "Influence of viscous dissipation and radiation on unsteady mhd mixed convection flow of micropolar fluids," *Applied Mathematics and Information Sciences*, vol. 2, pp. 143–162, 2008.
- [19] S. Mukhopadhyay, "Effect of thermal radiation on unsteady mixed convection flow and heat transfer over a porous stretching surface in porous medium," *International Journal of Heat and Mass Transfer*, vol. 52, pp. 3261–3265, 2009.
- [20] T. Fang, F. C. Lee, and J. Zhang, "The boundary layers of an unsteady incompressible stagnation-point flow with mass transfer," *International Journal of Nonlinear Mechanics*, vol. 46, pp. 942–948, 2011.
- [21] K. Bhattacharyya, "Heat transfer analysis in unsteady boundary layer stagnation-point flow towards a shrinking/stretching sheet," *Ain Shams Engineering Journal*, vol. 4, pp. 259–264, 2013.
- [22] H. I. Andersson, "Slip flow past a stretching surface," *Acta Mechanica*, vol. 158, pp. 121–125, 2002.
- [23] D. Pal and B. Talukdar, "Perturbation analysis of unsteady magnetohydrodynamic convective heat and mass transfer in a boundary layer slip flow past a vertical permeable plate with thermal radiation and chemical reaction," *Communications in Nonlinear Science and Numerical Simulation*, vol. 15, pp. 1813–1830, 2010.
- [24] S. Mukhopadhyay, "Slip effects on MHD boundary layer flow over an exponentially stretching sheet with suction/blowing and thermal radiation," *Ain Shams Engineering Journal*, vol. 4, pp. 485–491, 2013.
- [25] A. Aziz, J. I. Siddique, and T. Aziz, "Steady boundary layer slip flow along with heat and mass transfer over a flat porous plate embedded in a porous medium," *PLOS ONE*, 2014.
- [26] T. Hayat, A. Shafiq, A. Alsaedi, and S. A. Shahzad, "Unsteady mhd flow over exponentially stretching sheet with slip conditions," *Applied Mathematics and Mechanics*, vol. 37, no. 2, p. 193208, 2016.

- [27] F. C. Lai and F. A. Kulacki, "The effect of variable viscosity on convective heat transfer along a vertical surface in a saturated porous medium," *International Journal of Heat and Mass transfer*, vol. 33, pp. 1028–1031, 1990.
- [28] I. Pop, R. S. R. Gorla, and M. Rashidi, "The effect of variable viscosity on flow and heat transfer to a continuous moving flat plate," *International Journal of Engineering Science*, vol. 30, pp. 1–6, 1992.
- [29] T. C. Chiam, "Heat transfer with variable conductivity in a stagnation-point flow towards a stretching sheet," *International Communications in Heat and Mass Transfer*, vol. 32, pp. 239–248, 1996.
- [30] T. C. Chiam, "Heat transfer in a fluid with variable thermal conductivity over stretching sheet," *Acta Mechanica*, vol. 129, pp. 63–72, 1998.
- [31] S. Mukhopadhyay, G. C. Layek, and S. A. Samad, "Study of mhd boundary layer flow over a heated stretching sheet with variable viscosity," *International Journal of Heat and Mass Transfer*, vol. 48, pp. 4460–4466, 2005.
- [32] S. Mukhopadhyay and G. C. Layek, "Effects of variable fluid viscosity on flow past a heated stretching sheet embedded in a porous medium in presence of heat source/sink," *Meccanica*, vol. 47, pp. 863–876, 2012.
- [33] T. Hayat, S. A. Shehzad, M. Qasim, and A. Alsaedi, "Mixed convection by a porous sheet with variable thermal conductivity and convective boundary condition," *Brazilian Journal of Chemical Engineering*, vol. 31, pp. 109–117, 2014.
- [34] S. Choi, "Enhancing thermal conductivity of fluids with nanoparticles," in *ASME International Mechanical Engineering Congress and Exposition*, vol. 66, (San Francisco, California, USA), pp. 99–105, 1995.
- [35] J. Buongiorno, "Convective transport in nanofluids," *ASME Journal of Heat Transfer*, vol. 128, pp. 240–250, 2006.

- [36] J. A. Eastman, S. U. S. Choi, S. Li, W. Yu, and L. J. Thompson, “Anomalously increases effective thermal conductivities of ethylene glycol-bases nanofluids containing copper nanoparticles,” *Applied Physics Letters*, vol. 78, no. 6, 2001.
- [37] W. A. Khan and I. Pop, “Boundary-layer flow of a nanofluid past a stretching sheet,” *International Journal of Heat and Mass Transfer*, vol. 53, pp. 2477 – 2483, 2010.
- [38] O. Makinde and A. Aziz, “Boundary layer flow of a nanofluid past a stretching sheet with a convective boundary condition,” *International Journal of Thermal Sciences*, vol. 50, pp. 1326–1332, 2011.
- [39] R. Kandasamy, P. Loganathan, and P. P. Arasu, “Scaling group transformation for mhd boundary layer flow of a nanofluid past a vertical stretching surface in the presence of suction/injection,” *Nuclear Engineering and Design*, vol. 241, pp. 2053–2059, 2011.
- [40] K. Bhattacharyya and G. C. Layek, “Magnetohydrodynamic boundary layer flow of nanofluid over an exponentially stretching permeable sheet,” *Physics Research International*, 2014.
- [41] B. Shankar and Y. Yirga, “Unsteady heat and mass transfer in MHD flow of nanofluids over stretching sheet with a non-uniform heat source/sink,” *International Journal of Mathematical, Computational, Statistical, Natural and Physical Engineering*, vol. 7, pp. 1248 – 1256, 2013.
- [42] K. Das, P. R. Duari, and P. K. Kundu, “Nanofluid flow over an unsteady stretching surface in presence of thermal radiation,” *Alexandria Engineering Journal*, pp. 737–745, 2014.
- [43] T. G. Motsumi and O. D. Makinde, “Effects of the thermal radiation and viscous dissipation on boundary layer flow of nanofluids over a permeable strteching flat plate,” *Physica Scripta*, vol. 86, no. 4, 2012.

- [44] M. S. Khan, I. Karim, L. E. Ali, and A. Islam, “Unsteady MHD free convection boundary layer flow of a nanofluid along a stretching sheet with thermal radiation and viscous dissipation,” *International Nano Letters*, 2012.
- [45] A. Noghrehabadi, R. Pourrajab, and M. Ghalambaz, “Effect of partial slip boundary condition on the flow and heat transfer of nanofluids past stretching sheet prescribed constant wall temperature,” *International Journal of Thermal Sciences*, vol. 54, pp. 253–261, 2012.
- [46] S. Mansur and A. Ishak, “Unsteady boundary layer flow of a nanofluid over a stretching/shrinking sheet with a convective boundary condition,” *Egyptian Mathematical Society*, pp. 1–6, 2016.
- [47] L. Zheng, C. Zhanga, X. Zhang, and J. Zhang, “Flow and radiation heat transfer of a nanofluid over a stretching sheet with velocity slip and temperature jump in porous medium,” *Journal of the Franklin Institute*, vol. 350, pp. 990–1007, 2013.
- [48] M. uddin, I. Pop, and A. I. M. Ismail, “Free convection boundary layer flow of a nanofluid from a convectively heated vertical plate with linear momentum slip boundary condition,” *Sains Malaysiana*, vol. 4, no. 11, pp. 1475–1482, 2012.
- [49] W. Ibrahim and B. Shankar, “MHD boundary layer flow and heat transfer of a nanofluid past a permeable stretching sheet with velocity, thermal and solutal slip boundary conditions,” *Computers and Fluids*, vol. 75, pp. 1–10, 2013.
- [50] R. Sharma and A. Ishak, “Second order slip flow of cu-water nanofluid over a stretching sheet with heat transfer,” *WSEAS Transactions on Fluid Mechanics*, vol. 9, 2014.
- [51] K. Das, “Nanofluid flow over a non-linear permeable stretching sheet with partial slip,” *Journal of the Egyptian Mathematical Society*, vol. 23, pp. 451 – 456, 2015.
- [52] N. B. Reddy, T. Poornima, and P. Sreenivasulu, “Influence of variable thermal conductivity on mhd boundary layer slip flow of ethylene-glycol based cu nanofluids over a stretching sheet with convective boundary condition,” *International Journal of Engineering Mathematics*, 2014.

- [53] A. Noghrehabadi, M. Ghalambaz, and A. Ghanbarzadeh, “Effects of variable viscosity and thermal conductivity on natural convection of nanofluids past a vertical plate in porous media,” *Journal of Mechanics*, vol. 30, pp. 265–275, 2014.
- [54] a. W. A. K. Rashid Ahmad, “Unsteady heat and mass transfer MHD nanofluid flow over a stretching sheet with heat source/sink using quasi-linearization technique,” *Canadian Journal of Physics*, 2015.
- [55] N. Kishan, C. Kalyani, and M. C. K. Reddy, “Mhd boundary layer flow of a nanofluid over an exponentially permeable stretching sheet with radiation and heat source/sink,” *Transport phenomena in nano and micro scales*, vol. 4, Issue 1, Winter and Spring 2016, Page, pp. 44–51, 2016.
- [56] M. J. Uddin, W. Khan, and N. S. Amin, “G-Jitter mixed convective slip flow of nanofluid past a permeable stretching sheet embedded in a Darcian porous media with variable viscosity,” *PLOS ONE*, vol. 9, 2014.
- [57] E. Abu-Nada and A. J. Chamkha, “Effect of nanofluid variable properties on natural convection in enclosures filled with a CuO-EG-Water nanofluid,” *International Journal of Thermal Sciences*, vol. 49, pp. 2339–2352, 2010.
- [58] R. Nasrin and M. A. Alim, “Entropy generation by nanofluid with variable thermal conductivity and viscosity in a flat plate solar collector,” *International Journal of Engineering Science and Technology*, vol. 7, no. 2, pp. 80–93, 2015.
- [59] R. W. Fox, A. T. MacDonald, and P. J. Pritchard, *Introduction to Fluid Mechanics*. 7 ed., 2008.
- [60] J. Maxwell, *A Treatise on Electricity and Magnetism*. Oxford University Press, Cambridge, UK, 2nd ed., 1904.
- [61] A. Raptis, C. Perdakis, and H. S. Takhar, “Effect of thermal radiation on MHD flow,” *Applied Mathematics and Computation*, vol. 153, no. 3, pp. 645–649, 2004.

- [62] T. Hayat, M. Qasim, and S. Mesloub, “MHD flow and heat transfer over permeable stretching sheet with slip conditions,” *International Journal for Numerical Methods in Fluids*, vol. 66, pp. 963–975, 2011.